



VOL. 367 PB

1 December 2022

ISSN 0167-7322

journal of MOLECULAR LIQUIDS

Structure, Interactions and Dynamics of Simple,
Molecular, Ionic and Complex Liquids

Editors-in-Chief

A. Valente (Universidade de Coimbra, Coimbra, Portugal)
L. Vega (Khalifa University, Abu Dhabi, United Arab Emirates)
T. Yamaguchi (Fukuoka University, Fukuoka, Japan)

www.elsevier.com/locate/molliq



ScienceDirect®

Journal of Molecular Liquids

Supports *open access*

9

CiteScore

6.633

Impact Factor

[Submit your article](#)[Guide for authors](#)

Menu

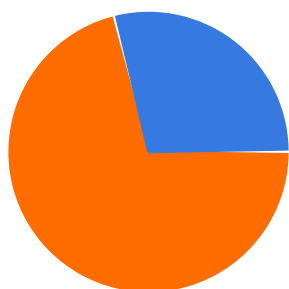


Search in this journal

[> Aims and scope](#)[> Editorial board](#)[> Abstracting & indexing](#)[> Call for papers](#)[> News](#)[> Conferences](#)

Gender diversity of editors

Based on 100.00% responding editors



71% man

FEEDBACK

29% woman

0% non-binary or gender diverse

0% prefer not to disclose

Editorial board by country/region

41 editors and editorial board members in 20 countries/regions

1 Germany (5)

2 India (5)

3 France (4)

[> See more editors by country/region](#)

Editorial board

Editors in Chief



T. Yamaguchi, PhD

Fukuoka University Faculty of Science Graduate School of Science Department of Chemistry,
Nanakuma, Jonan-ku, 814-0180, Fukuoka, Japan

[> View full biography](#)

[Email this editor](#) ↗



J.M. Valente, PhD / Dr.

University of Coimbra Department of Chemistry, Rua Larga, 3004-535, Coimbra, Po

FEEDBACK

[View full biography](#)

[Email this editor](#) ↗

L. F. Vega

Khalifa University, 127788, Abu Dhabi, United Arab Emirates

[View full biography](#)

[Email this editor](#) ↗

Editors

M. Bešter-Rogač

University of Ljubljana Faculty of Chemistry and Chemical Technology, Ljubljana, Slovenia

[View full biography](#)

F. Llorell

Rovira i Virgili University Department of Chemical Engineering, Tarragona, Spain

[View full biography](#)

F.W. Tavares

Federal University of Rio de Janeiro, Rio de Janeiro, Brazil

[View full biography](#)

P. Venkatesu

University of Delhi Department of Chemistry, New Delhi, India

[View full biography](#)

Z. W. Yu

Department of Chemistry, Key Laboratory Of Bioorganic Phosphorus Chemistry & Chemical Biology, Ministry of education, Tsinghua University, Beijing, China

[View full biography](#)

Emeritus Editor

W. Schröer

University of Bremen Faculty 2 Biology Chemistry, Bremen, Germany

Editorial Board

H. Abramczyk

Lodz, Poland

A. Apelblat

Be'er Sheva, Israel

B. Bagchi

Bengaluru, India

J. Barthel

Regensburg, Germany

M.C. Bellisent-Funel

Gif sur Yvette, France

P. Bojarski, Ph.D., D.Sc.

Gdańsk, Poland

[View full biography](#)

P.A. Bopp

Talence CEDEX, France

R. Buchner, PhD

Regensburg, Germany

A. Chandra

Kanpur, India

G. Douheret

Vichy, France

V. Durov

Moskva, Russian Federation



R. L. Gardas, PhD

Chennai, India

[View full biography](#)

A. Geiger

Dortmund, Germany

J. Glinski

Wroclaw, Poland

P. Grigolini

Denton, Texas, United States of America

G.T. Hefter

Murdoch, Australia

J.T. Hynes

Boulder, Colorado, United States of America

A. Idrissi

Villeneuve d'Ascq, France

Jedlovszky, Ph. D., D. Sc.

Eger, Hungary

A. Lauberau

Garching, Germany

Y. Marcus

Jerusalem, Israel

M. Maroncelli

University Park, Pennsylvania, United States of America

N.O. Mchedlov-Petrosyan

Kharkiv, Ukraine

R. Novakovic

Genova, Italy



J. Samios

Athens, Greece

Z.A. Schelly

Arlington, Texas, United States of America



R.J. Sengwa, Ph.D.

Jodhpur, India

[View full biography](#)

T. Takamuku, Dr.

Saga, Japan

R. Vallauri

Trento, Italy

S. Velasco

Salamanca, Spain



X. Wang, PhD

Beijing, China

[View full biography](#)

H. Weingaertner

Bochum, Germany

J. Yarwood

Sheffield, United Kingdom

All members of the Editorial Board have identified their affiliated institutions or organizations, along with the corresponding country or geographic region. Elsevier remains neutral with regard to any jurisdictional claims.

FEEDBACK 



Copyright © 2022 Elsevier B.V. or its licensors or contributors.
ScienceDirect® is a registered trademark of Elsevier B.V.





ScienceDirect®

[Submit your article](#)[Menu](#)[Search in this journal](#)

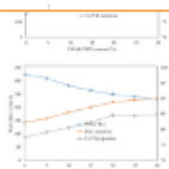
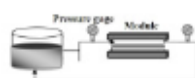
Volume 317

1 November 2020

[◀ Previous vol/issue](#)[Next vol/issue ▶](#)

Receive an update when the latest issues in this journal are published

[Sign in to set up alerts](#)[Full text access](#)[Editorial Board](#)[Article 114402](#)[📄 Download PDF](#)[Review](#)[Review article](#) ○ [Abstract only](#)[FEEDBACK](#)



☒ Research article ☐ Abstract only

Comparing natural and synthetic polymeric nanofluids in a mid-permeability sandstone reservoir condition

Augustine Agi, Radzuan Junin, Afeez Gbadamosi, Muhammad Manan, ... Faruk Yakasai

Article 113947

Article preview

Abstract

Abstract

Biopolymeric nanofluids have been proposed as an eco-friendly substitute to synthetic polymeric nanofluids to cut cost and environmental effect. However, previous studies on the use of biopolymeric nanofluids to enhance oil recovery focused only on adsorption and fluid injectivity at ambient condition. In this study, the thermal degradation of crystalline starch nanofluid (CSNF) at reservoir condition was investigated and compared with silica and aluminium oxide polymeric nanofluids, SiO₂PNF and Al₂O₃PNF respectively. The thermal degradation of the polymeric nanofluids was investigated using Brookfield RST rheometer. Moreover, interfacial tension (IFT) properties and wettability alteration efficiency of the polymeric nanofluids were determined using Easy Dyne KRUS tensiometer and sessile drop technique, respectively. Finally, the oil displacement ability of the polymeric nanofluids at typical reservoir condition was studied using Fars EOR technologies high-pressure high-temperature apparatus. Experimental result shows that the viscosities of SiO₂PNF and Al₂O₃PNF decreased with increase in

☐ Research article ☐ Abstract only

Measuring solubility of a chemotherapy-anti cancer drug (busulfan) in supercritical carbon dioxide

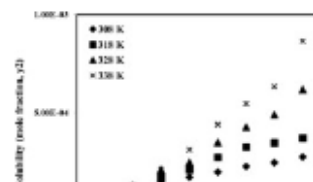
Mahboubeh Pishnamazi, Samyar Zabihi, Sahar Jamshidian, Hoda Zeinolabedin Hezaveh, ... Saeed Shirazian

Article 113954

Article preview

Abstract Graphical abstract

Graphical abstract



[Submit your article](#)[Menu](#)[Search in this journal](#)[Abstract](#)

Abstract

As a new type of energy storage technology, latent heat energy storage (LHTES) has the advantages of high energy density and energy efficiency. Compared with inorganic phase change materials (PCMs) having supercooling (SC) and phase separation, the composite PCMs of inorganic and organic materials can expand the application range of single PCMs. It is found that PCH often occurs in the phase transition of composite PCMs. PCH is the temperature delay between the melting and solidification process, and SC means that solidification does not start at the nominal solidification temperature and a lower temperature is needed for the nucleation to start. In this paper, the enthalpy method and the effective heat capacity method are analyzed. Then the modeling approaches and experimental studies on

Regular Papers

[Research article](#) [Open access](#)

CFD approach for simulation of API release from solid dosage formulations

Jordan P. Walsh, Mahdi Ghadiri, Saeed Shirazian

Article 113899

[Download PDF](#) [Article preview](#)[Abstract](#)[Graphical abstract](#)

Graphical abstract

[FEEDBACK](#)

[Submit your article](#)[Menu](#)[Search in this journal](#)[Research article](#) ☐ [Abstract only](#)

Determination and correlation of solubility of 4,4'-difluorobenzophenone in pure and binary mixed solvents and thermodynamic properties of solution

Mingyan Li, Zidan Gao, Zhili Li, Zhirong Wang, ... Baohua Wang

Article 113903

[Purchase PDF](#) [Article preview](#)

Abstract

Abstract

The target of this study was to determine and correlate the solubility of 4,4'-difluorobenzophenone in various solvents from 293.15 K to 333.15 K by gravimetric method at 0.1 MPa, and at the same time got the thermodynamic parameters. In this work, methanol, ethanol, *n*-propanol, isopropanol, *n*-butanol, isobutanol, ethyl acetate, methyl acetate, acetone, acetonitrile pure solvents and ethanol + *n*-propanol mixed solvents were selected as the experimental solvents. The results showed that the solubility of 4,4'-difluorobenzophenone in selected solvents increased with increasing temperature within the investigated temperature range. The effect of solvent properties on 4,4'-difluorobenzophenone solubility behaviors was discussed by solvent polarity, hydrogen bonding donor and acceptor propensity and cohesive

[Research article](#) ☐ [Abstract only](#)

Surface properties and microemulsion of anionic/nonionic mixtures based on sulfonate Gemini surfactant in the presence of NaCl

Jing Wu, Ping Mei, Juan Wu, Jun-Wei Fu, ... Lu Lai

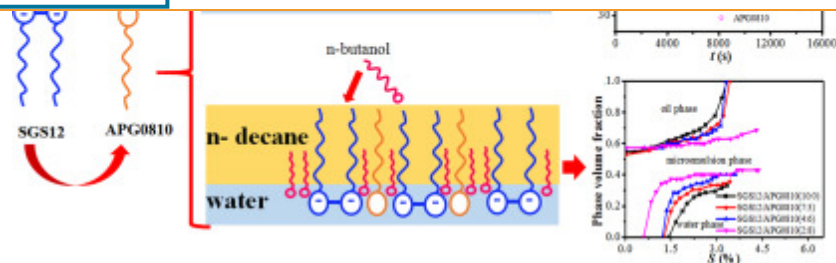
Article 113907

[Purchase PDF](#) [Article preview](#)[FEEDBACK](#)

Menu



Search in this journal



Research article ○ Abstract only

Steric effect in the formation of hydrogen bonded complexes of isopropylamine with alicyclic ethers by ultrasonic and DFT approach

S.G. Mohammed Hussain, R. Kumar, M. Mohamed Naseer Ali, V. Kannappan

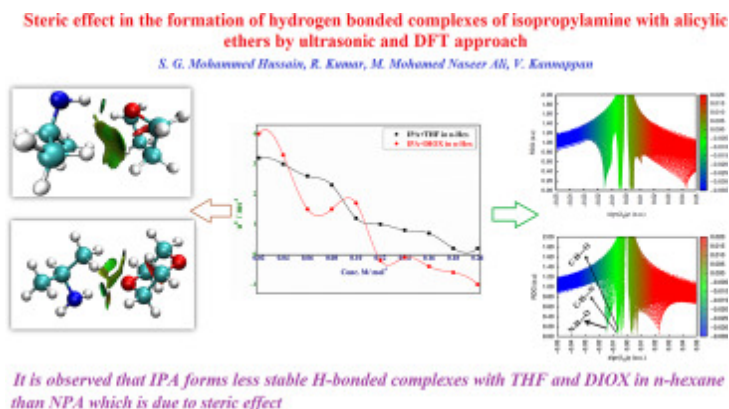
Article 113910

[Purchase PDF](#) Article preview

Abstract

Graphical abstract

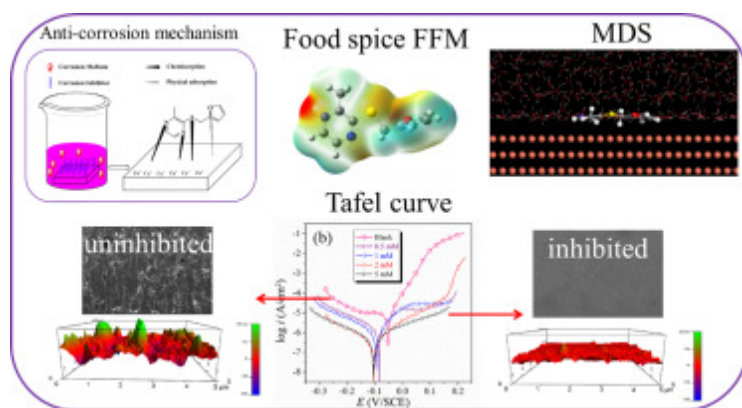
Graphical abstract



Research article ○ Abstract only

[Submit your article](#)[Menu](#)[Search in this journal](#)[Abstract](#)[Graphical abstract](#)

Graphical abstract



Research article ○ Abstract only

Design and synthesis of a novel corrosion inhibitor embedded with quaternary ammonium, amide and amine motifs for protection of carbon steel in 1 M HCl

Dheeraj Singh Chauhan, Mumtaz A. Quraishi, Mohammad A. Jafar Mazumder, Shaikh A. Ali, ... Bader G. Alharbi

Article 113917

[Purchase PDF](#) [Article preview](#)[Abstract](#)[Graphical abstract](#)

Graphical abstract

[FEEDBACK](#)

Journal of Molecular Liquids

Supports open access

Submit your article

Menu



Search in this journal

Can CHARMM36 atomic charges described correctly the interaction between amino acid and water molecules by molecular dynamics simulations?

Leonardo Bruno Assis Oliveira, Guilherme Colherinhas

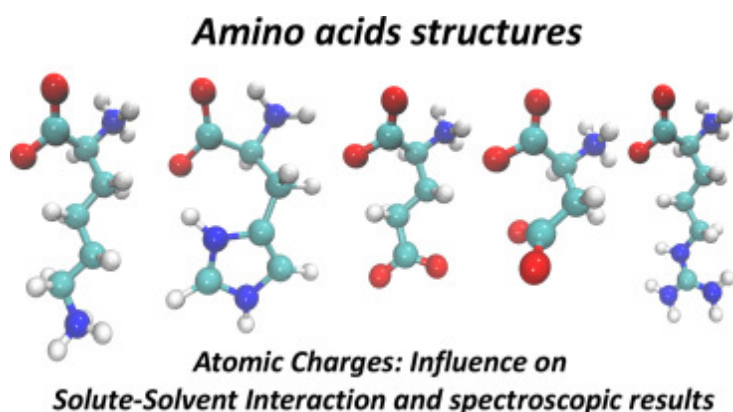
Article 113919

[Purchase PDF](#) Article preview

Abstract

Graphical abstract

Graphical abstract



Research article ○ Abstract only

Chromatographic and UV–visible spectrophotometric pK_a determination of some purine antimetabolites

Y. Doğan Daldal, Ebru Çubuk Demiralay

Article 113930

[Purchase PDF](#) Article preview

Abstract

Graphical abstract

Graphical abstract

FEEDBACK

[Submit your article](#)[Menu](#)[Search in this journal](#)[Research article](#) ○ [Abstract only](#)

Developing NaAc•3H₂O-based composite phase change material using glycine as temperature regulator and expanded graphite as supporting material for use in floor radiant heating

Wanwan Fu, Yuting Lu, Rongtang Zhang, Jiesheng Liu, Tongtong Zhang

Article 113932

[Purchase PDF](#) [Article preview](#)

Abstract

Abstract

Floor radiant heating embedded phase change materials (PCMs) are a prospective field owing to its highly efficient energy-saving effect and comfortable thermal environment. In this work, using a non-eutectic mixture comprised of NaAc•3H₂O (main PCM) and glycine (temperature regulator) as PCM, and expanded graphite (EG) as supporting material, a novel composite PCM with high thermal performance used in the heat exchanger for the floor radiant heating was developed. The composition of the composite PCM was optimized, and its properties were studied. The results showed that the mixture containing 12% glycine was favorable due to its suitable phase change temperature (48.62 °C) and high phase change enthalpy (258.5 kJ·kg⁻¹). The addition of 12% EG into the mixture could enhance thermal conductivity and prevent

[Research article](#) ○ [Abstract only](#)

A combined molecular dynamics and quantum mechanics study on the interaction of Fe³⁺ and human serum albumin relevant to iron overload disease

Sadegh Kaviani, Mohammad Izadyar, Mohammad Khavani, Mohammad Reza Housaindokht

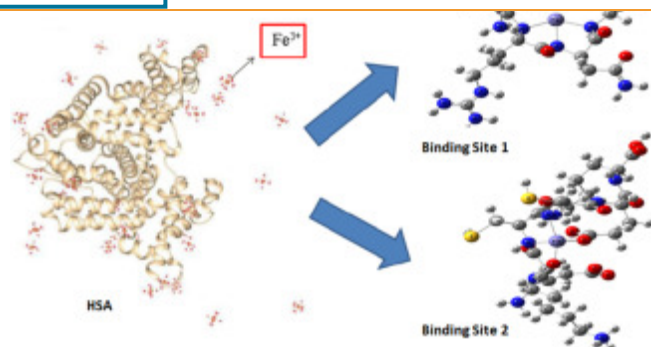
Article 113933

[FEEDBACK](#)

Menu



Search in this journal



Research article ○ Abstract only

Metal organic framework nanoparticles loaded- PVDF/chitosan nanofibrous ultrafiltration membranes for the removal of BSA protein and Cr(VI) ions

Mohammad Pishnamazi, Shahnaz Koushkbaghi, Seiede Samira Hosseini, Meisam Darabi, ... Mohammad Irani

Article 113934

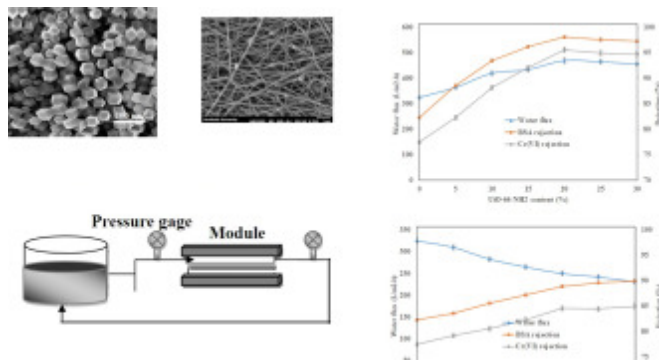
[Purchase PDF](#) Article preview [Article preview](#)

Abstract

Graphical abstract

Graphical abstract

The performance of MOF loaded ultrafiltration nanofibrous membrane for rejection of BSA and Cr(VI).



FEEDBACK

Menu



Search in this journal

[Purchase PDF](#) [Article preview](#)

Research article ○ Abstract only

Measuring solubility of a chemotherapy-anti cancer drug (busulfan) in supercritical carbon dioxide

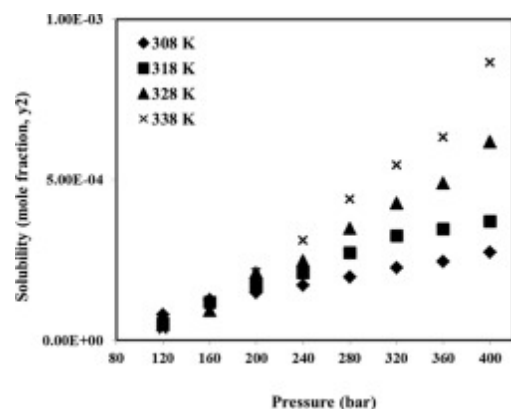
Mahboubeh Pishnamazi, Samyar Zabihi, Sahar Jamshidian, Hoda Zeinolabedin Hezaveh, ... Saeed Shirazian

Article 113954

[Purchase PDF](#) [Article preview](#)

Abstract Graphical abstract

Graphical abstract



Research article ○ Abstract only

Evaluation of mesomorphic and thermal stabilities for terminal epoxy liquid crystals

Shengbo Zhu, Wei Li, Bingyang Lu, Weixing Chen, ... Zhongwei An

Article 113955

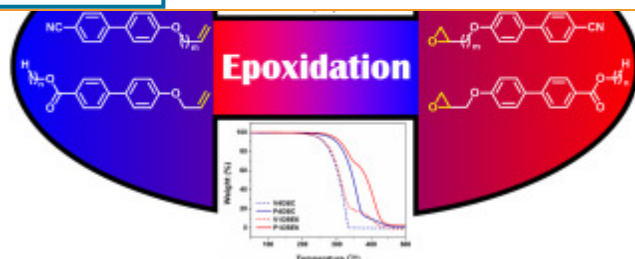
[Purchase PDF](#) [Article preview](#)

Submit your article

Menu



Search in this journal



Research article ○ Abstract only

Electrical conductivity of ion-doped fluoro substituted liquid crystal compounds for application in the dynamic light scattering effect

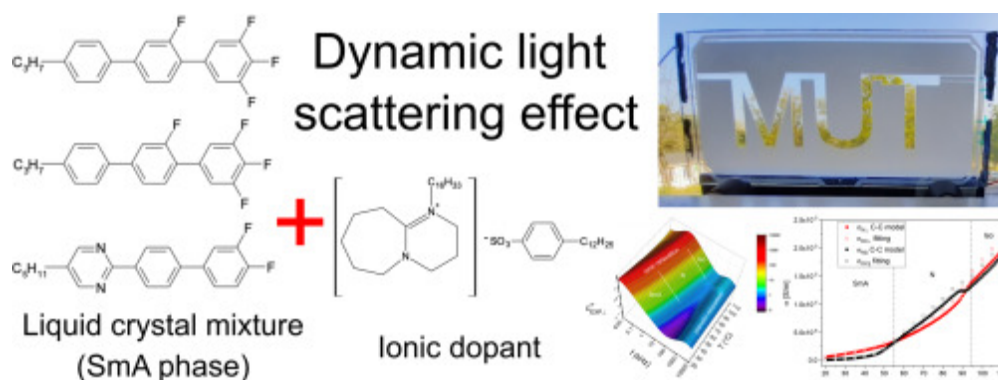
Mateusz Mrukiewicz, Paweł Perkowski, Magdalena Urbańska, Dorota Węglowska, Wiktor Piecek
Article 113810

[Purchase PDF](#) Article preview [Article preview](#)

Abstract

Graphical abstract

Graphical abstract



Research article ○ Abstract only

FEEDBACK

[Submit your article](#)[Menu](#)[Search in this journal](#)

Abstract

Abstract

In this paper we study the complexation of Al^{3+} and several transition metals (Cr^{3+} , Fe^{3+} , Mn^{2+} , Ni^{2+}) in the ionic liquid 1-butyl-3-methylimidazolium thiocyanate. New insights into the structure, single-particle dynamics and electronic properties (optical absorption spectra) of these bulk mixtures are provided by molecular dynamics and density functional theory calculations, and our results are successfully compared with available experimental data. Our theoretical results reveal the existence of a bridging coordination mode between neighboring metal-ligand complexes in the polar nanoregions, and a scarce influence of the apolar nanoregions in the single-particle dynamics of the species in the mixture. Moreover, most part of the relevant features of the UV–Vis optical absorption spectra of these systems is properly

Research article ○ Abstract only

From pan-genome to protein dynamics: A computational hierarchical quest to identify drug target in multi-drug resistant *Burkholderia cepacia*

Faisal Ahmad, Syed Sikander Azam

Article 113904

[Purchase PDF](#) Article preview [↗](#)

Abstract

Graphical abstract

Graphical abstract

[FEEDBACK](#)

Journal of Molecular Liquids

Supports *open access*

Submit your article

Menu



Search in this journal

Research article ○ Abstract only

Crystal polymorphs in 1-alkyl-3-methylimidazolium perfluorobutanesulfonate ionic liquids

Yoshihiro Koyama, Seiya Shimono, Hiroshi Abe, Kiyoto Matsuishi

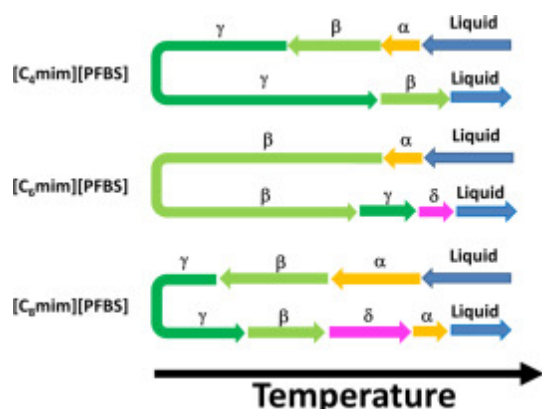
Article 113908

[Purchase PDF](#) Article preview [^](#)

Abstract

Graphical abstract

Graphic abstract



Research article ○ Abstract only

Molecular modeling insights in the extraction of benzene from hydrocarbon stream using deep eutectic solvent

Nikhil Kumar, Papu Kumar Naik, Tamal Banerjee

Article 113909

[Purchase PDF](#) Article preview [^](#)

Abstract

Graphical abstract

FEEDBACK

Submit your article

Menu



Search in this journal

[Erratum](#) [Full text access](#)

Corrigendum

Neha Chaudhary, Anil Kumar Nain

Article 113912

[Download PDF](#)Research article ☐ Abstract only

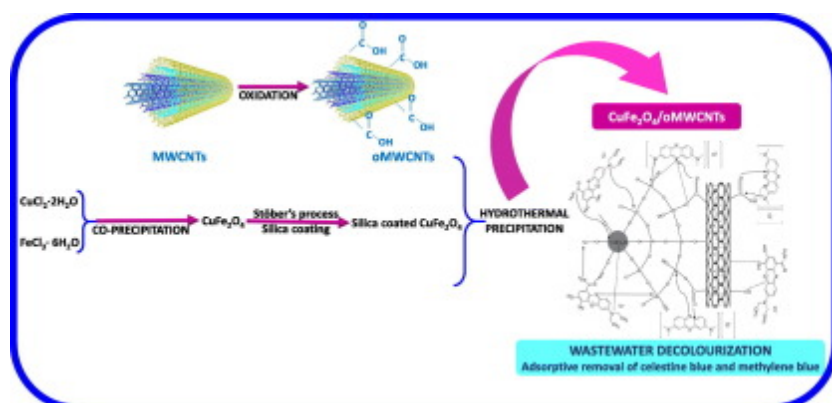
Oxygenated functionalities enriched MWCNTs decorated with silica coated spinel ferrite – A nanocomposite for potentially rapid and efficient de-colorization of aquatic environment

Saikh Mohammad Wabaidur, Moonis Ali Khan, Masoom Raza Siddiqui, Marta Otero, ... Afnan Ali Hussain Hakami

Article 113916

[Purchase PDF](#) [Article preview](#)[Abstract](#)[Graphical abstract](#)

Graphical abstract



FEEDBACK

Submit your article

Menu



Search in this journal

Andrey A. Toropov, Natalia Sizchenko, Anna I. Toropova, Danuta Leszczynska, Jerzy Leszczynski

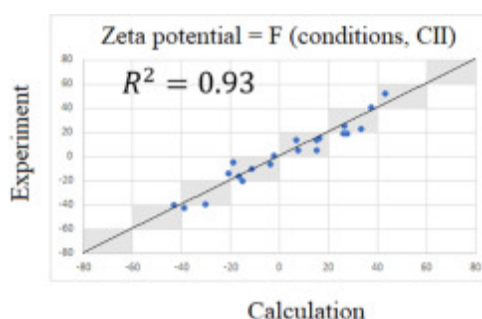
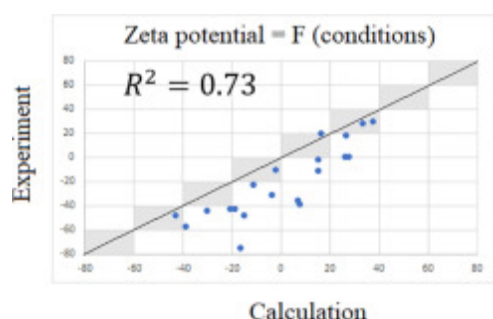
Article 113929

[Purchase PDF](#) Article preview

Abstract

Graphical abstract

Graphical abstract



Research article ○ Abstract only

Quantum chemical prediction of the spectroscopic properties and ionic composition of the molten NaF-AlF₃ salts

Min Tan, Tao Li, Bo Shang, Henan Cui

Article 113937

[Purchase PDF](#) Article preview

Abstract

Abstract

The behavior of the ions in the molten NaF-AlF₃ salts plays a significant role in aluminium reduction process. Many experimental and modelling works have been carried out to investigate the ionic composition of the molten cryolite, which are still controversial. In this study, a recent thermodynamic model was introduced to compare with the Temkin model,

FEEDBACK

[Submit your article](#)[Menu](#)[Search in this journal](#)[Research article](#) ☐ [Abstract only](#)

The effects of zero and high shear rates viscosities on the transportation of heat and mass in boundary layer regions: A non-Newtonian fluid with Carreau model

Mohsan Hassan, Alibek Issakhov, Salah Ud-Din Khan, Mamdouh El Haj Assad, ... Shahab Ud-Din Khan
Article 113991

[Purchase PDF](#) [Article preview](#)

Abstract

Abstract

The momentum and thermal boundary layer flow problem for shear thinning fluid with modified viscosity model over moving wedge is discussed. The mathematical model of the problem is developed by using improved Carreau model relates viscosity to shear rate and using the thermal conductivity model in the similar form of viscosity expression. The improved Carreau model contains five-parameters: zero viscosity, high shear rate viscosity, flow behavior index, consistency index and viscosity curvature which cover almost all aspects of the fluid's rheology. On the governing equations of the problem, boundary layer approximations are used and then reduced into ordinary differential equations by using similarity transformations. The results in form of velocity and temperature profiles, thickness of

[Research article](#) ☐ [Abstract only](#)

Sugar-based natural deep eutectic solvents as potential absorbents for NH₃ capture at elevated temperatures and reduced pressures

Zi-Liang Li, Fu-Yu Zhong, Ji-Yong Huang, Hai-Long Peng, Kuan Huang
Article 113992

[Purchase PDF](#) [Article preview](#)

Abstract

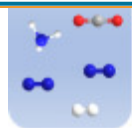
Graphical abstract

[FEEDBACK](#)

Menu



Search in this journal



Research article ○ Abstract only

Organic-inorganic microspheres of temperature-controlled size for profile control

Ling Liu, Shaohua Gou, Shenwen Fang, Yang He, Lan Tang

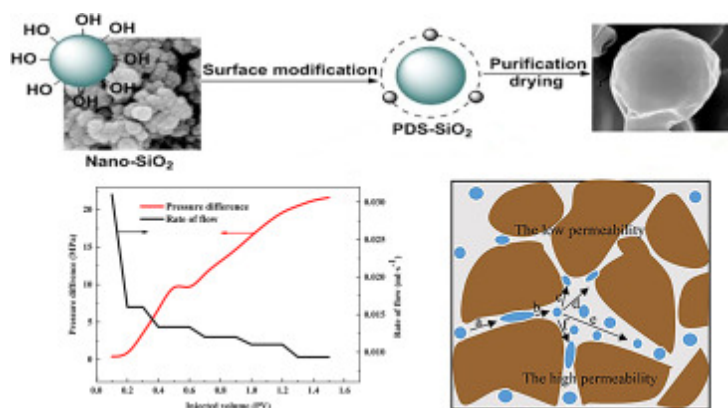
Article 113993

[Purchase PDF](#) Article preview

Abstract

Graphical abstract

Graphical abstract



Research article ○ Abstract only

Thermodynamics of tetramethylurea solutions in ethylene glycol: The evidence of pairwise solvophobic interaction

Evgeniy V. Ivanov, Andrey V. Kustov, Dmitriy V. Batov, Natalia L. Smirnova, Nadezhda L. Pechnikova

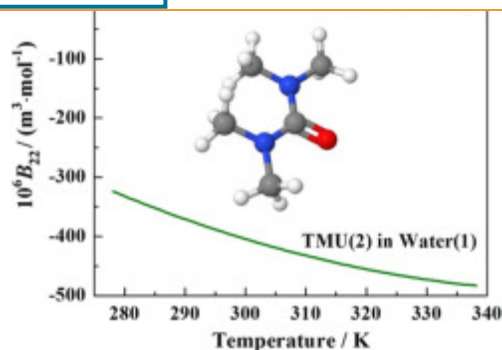
Article 113994

FEEDBACK

Menu



Search in this journal



Research article ○ Abstract only

Influence of the oxidation rate on the dielectric properties of water confined in graphene bilayers

Haochen Zhu, Bo Hu, Han Hu, Yunjie Zhu, ... Guangming Li

Article 113995

[Purchase PDF](#) Article preview

Abstract

Abstract

In recent years, numerous studies have focused on enhancing water permeability and ion retention by oxidizing pristine graphene membranes. Despite advanced modification and successful applications, the physical properties involved in the separation processes by graphene oxide nanochannels, such as the dielectric constant are not fully understood. A series of molecular dynamics simulations are carried out in this work to investigate the dielectric properties of aqueous solution in both pristine and oxidized bilayer graphene membranes. Results show that the dielectric constant decreases with the increase of the oxidation ratio as the oxidation ratio of the channel is less than 20%. However, the dielectric properties violate the previous trend as the oxidation rate continues to increase up to 40%. We show that the

Submit your article

Menu



Search in this journal



Purchase PDF

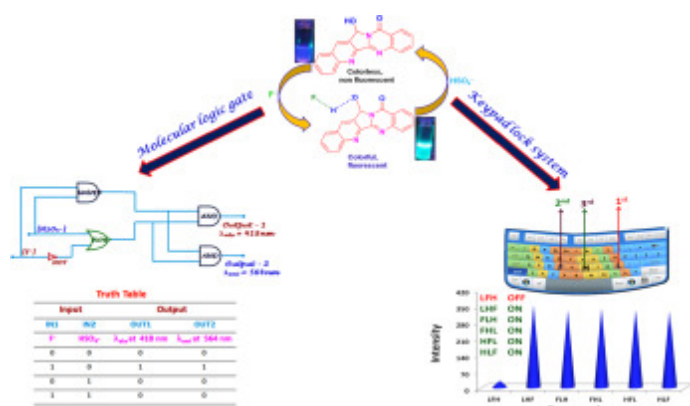
Article preview



Abstract

Graphical abstract

Graphical abstract



Research article ○ Abstract only

Laser diagnostics of self-organization of amphiphiles in aqueous solutions on the example of sodium octanoate

Ivan V. Plastinin, Sergey A. Burikov, Tatiana A. Dolenko

Article 113958



Purchase PDF

Article preview



Abstract

Graphical abstract

Graphical abstract

FEEDBACK

[Submit your article](#)[Menu](#)[Search in this journal](#)[Research article](#) ☐ [Abstract only](#)

Development of Abraham model correlations for short-chain glycol-grafted imidazolium and pyridinium ionic liquids from inverse gas-chromatographic measurements

Fabrice Mutelet, Gary A. Baker, Hua Zhao, Brittani Churchill, William E. Acree
Article 113983

[Purchase PDF](#) [Article preview](#)

Abstract

Abstract

Infinite dilution activity coefficients and gas-to-liquid partition coefficients are herein reported for more than 45 organic solutes of varying polarity and hydrogen-bonding character dissolved within the ether-grafted ionic liquids 1-ethyl-3-(2-methoxyethyl)imidazolium bis(trifluoromethylsulfonyl)imide and N-(2-methoxyethyl)pyridinium bis(trifluoromethylsulfonyl)imide. Experimental values were determined in 10 K intervals from 323.15 to 373.15 K using the method of inverse gas chromatography. Measured infinite dilution activity coefficients were then used to determine the partial molar excess Gibbs free energies, enthalpies, and entropies associated with the dissolution of these model solutes into these two short-chain glycol-grafted ionic liquids. Finally, based on the measured infinite dilution

[Research article](#) ☐ [Abstract only](#)

Physical origin of Na^+/Cl^- selectivity of tight junctions between epithelial cells. Nonlocal electrostatic approach

A.A. Rubashkin, P. Iserovich, M.A. Vorotyntsev
Article 113884

[Purchase PDF](#) [Article preview](#)[FEEDBACK](#)



strong difference in the permeabilities of these channels for Na^+ and Cl^- ion migrational fluxes owing to specific properties of the protein network inside TJs. It has been assumed in this study that this phenomenon originates from combination of two effects related to this specific TJ protein (claudin) which segments are partially located inside the TJ space. First, their ionogenic groups create a negative charge distributed inside TJs, thus inducing a difference between the Na^+ and Cl^- concentrations inside this spatial region. Second, the effect of these negative charges is greatly enhanced owing to high energetic barriers for penetration of both

Research article ○ Abstract only

Physical and transport properties of ionic liquids using geometric similitude and a cubic equation of state. Part 2: Thermal conductivity, and speed of sound of water + ionic liquid mixtures

Luis F. Cardona, José O. Valderrama

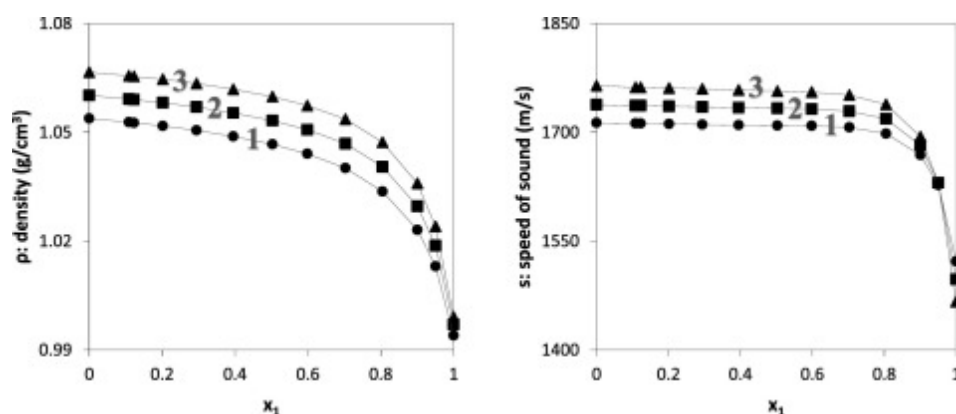
Article 113926

[Purchase PDF](#) Article preview

Abstract

Graphical abstract

Graphical abstract



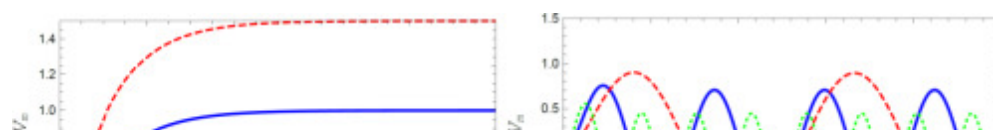
Research article ○ Abstract only

FEEDBACK

[Submit your article](#)[Menu](#)[Search in this journal](#)[Abstract](#) [Graphical abstract](#)

Graphical abstract

The figures illustrate the effect of constant and sinusoidal electric forces on the mean velocity $V(t)$ of the charged Brownian particle in a bath of other particles. The bath response to the external force affects neither the memory of the system described by the generalized Langevin equation nor the Kubo's fluctuation-dissipation theorem. However, $V(t)$ may substantially depend on whether (red and green lines) or not (blue line) the surroundings feel the external field.

[Research article](#) ☐ [Abstract only](#)

A sandwich electrochemical immunosensor based on antibody functionalized-silver nanoparticles (Ab-Ag NPs) for the detection of dengue biomarker protein NS1

Maryam Awan, Sajid Rauf, Azhar Abbas, Mian Hasnain Nawaz, ... Akhtar Hayat

Article 114014

[Purchase PDF](#) [Article preview](#)[Abstract](#) [Graphical abstract](#)

Graphical abstract

[FEEDBACK](#)

Journal of Molecular Liquids

Supports *open access*

Submit your article

Menu



Search in this journal

298.15 K and at 0.1 MPa

Kunal R. Patil, Shrikant P. Musale, Dilip H. Dagade

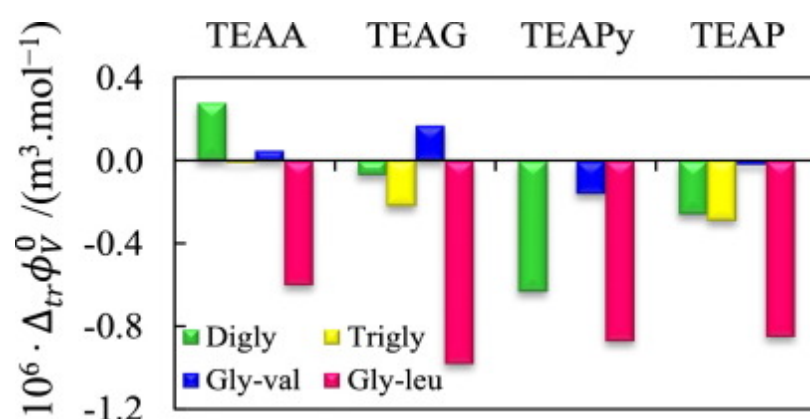
Article 113943

[Purchase PDF](#) Article preview

Abstract

Graphical abstract

Graphical abstract



Research article ○ Abstract only

Detecting pH and Ca^{2+} increase during low salinity waterflooding in carbonate reservoirs: Implications for wettability alteration process

Yongqiang Chen, Amir Ubaidah, Yogarajah Elakneswaran, Vahid J. Niasar, Quan Xie

Article 114003

[Purchase PDF](#) Article preview

Abstract

Abstract

FEEDBACK

[Submit your article](#)[Menu](#)[Search in this journal](#)[the effects of salinity level on calcite dissolution and pH increase against the recovery factor](#)Research article ☐ Abstract only

Molecular level insight into stability, activity, and structure of Laccase in aqueous ionic liquid and organic solvents: An experimental and computational research

Majid Jafari, Somayeh Mojtabavi, Mohammad Ali Faramarzi, Faramarz Mehrnejad, ... Rohollah Mirjani
Article 113925

[Purchase PDF](#) [Article preview](#)

Abstract

Abstract

Herein, we performed meticulous experimental and computational studies to explore the stability, activity, and dynamics of laccase in the presence of various organic and inorganic solvents. It is well known that laccases are eco-friendly enzymes, which can quickly eliminate recalcitrant chemicals from contaminated media. We determined the Asp96 (COO⁻)---Arg43 (N-H2), Asp131 (COO⁻)---Arg197(N-H1), Asp138(COO⁻)---Arg195 (N-H2), Asp140(COO⁻)---Arg199(N-H2), Asp214(COO⁻)---Arg260(N-H2), Asp224(COO⁻)---Arg423(N-H2), Asp424(COO⁻)---Arg243(N-H1), Asp424(COO⁻)---Arg243(N-H2), Glu288(COO⁻)---Arg176(N-H1) and Glu288(COO⁻)---Arg176(N-H2) salt bridges as the crucial ones in maintaining the structural integrity of laccase. Furthermore, the fluorescence, circular dichroism (CD) spectroscopies, and

Research article ☐ Abstract only

Theoretical and experimental studies of ionic liquid-urea mixtures on chitosan dissolution: Effect of cationic structure

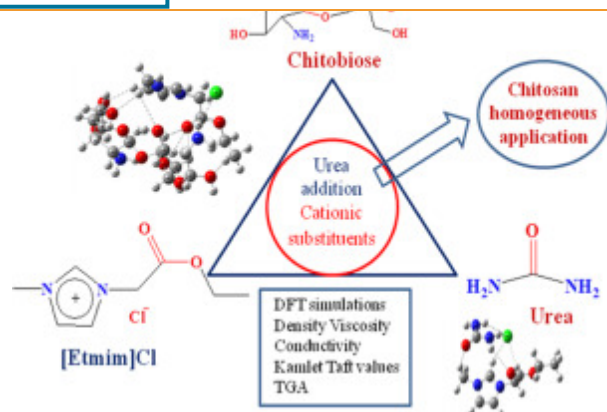
Linghua Zhuang, Fei Zhong, Mengyi Qin, Yu Sun, ... Guowei Wang
Article 113918

[FEEDBACK](#)

Menu



Search in this journal



Research article ○ Abstract only

Solubilization of hydrophobic drugs clozapine and oxcarbazepine in the lower and higher molecular weight pluronic mixed micelles-a physicochemical, *In vitro* release and *In vitro* anti-oxidant study

Pankaj Singla, Saweta Garg, Rajbir Bhatti, Marloes Peeters, ... Rakesh Kumar Mahajan

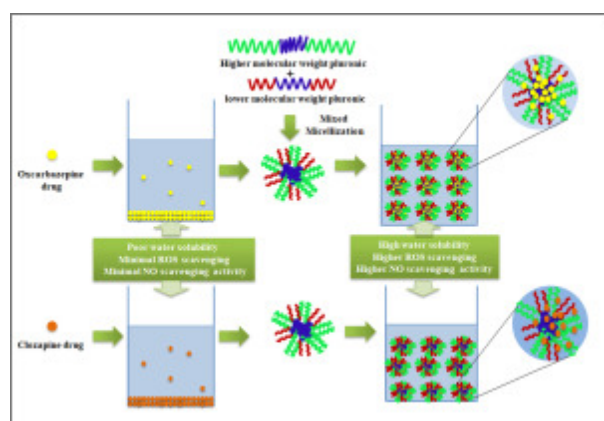
Article 113816

[Purchase PDF](#) Article preview [Article preview](#)

Abstract

Graphical abstract

Graphical abstract



[Submit your article](#)[Menu](#)[Search in this journal](#)[Purchase PDF](#)[Article preview](#)

Abstract

Abstract

The thermophysical properties of biodiesel surrogates are of great importance for the development of the new and clean fuel substitutes or additives. Experimental investigation and molecular dynamic simulation of the related thermophysical properties such as the liquid density, kinematic viscosity and surface tension over a sufficient wide temperature range will facilitate the corresponding researches of selecting the proper fuel surrogates and designing the spray system of the internal combustion engine. Therefore, the present study investigated liquid surface tension and kinematic viscosity of the proposed physical biodiesel surrogates of n-hexadecane with ethyl hexanoate and ethyl heptanoate by the surface light scattering method at three mole fractions (0.25, 0.50 and 0.75) over the temperature range from (353.15 to 433.15)

Research article ○ Abstract only

Benzidine-based Schiff base compounds for employing as corrosion inhibitors for carbon steel in 1.0 M HCl aqueous media by chemical, electrochemical and computational methods

M.A. Bedair, S.A. Soliman, Mostafa F. Bakr, E.S. Gad, ... Faleh Z. Alqahtany

Article 114015

[Purchase PDF](#)[Article preview](#) [Abstract](#)[Graphical abstract](#)

Graphical abstract

[FEEDBACK](#)

Submit your article

Menu



Search in this journal

Research article ○ Abstract only

Development of mercaptosuccinic anchored MOF through one-step preparation to enhance adsorption capacity and selectivity for Hg(II) and Pb(II)

Chen Wang, Guo Lin, Yunhao Xi, Xiteng Li, ... Libo Zhang

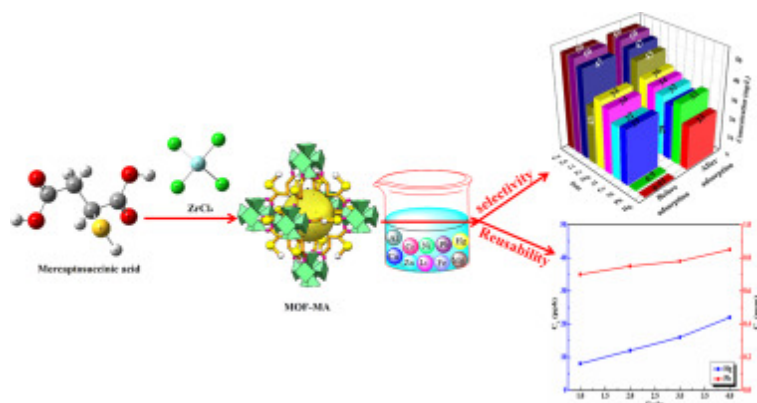
Article 113896

[Purchase PDF](#) Article preview

Abstract

Graphical abstract

Graphical abstract



Research article ○ Abstract only

Influence of PVP-PEG mixed aggregates and electrolytes on the rate of alkaline hydrolysis of benzocaine in aqueous and surfactant medium

Farheen Rahman, Mohd Sajid Ali, H.A. Al-Lohedan, Elham Aazam, ... M.Z.A. Rafiquee

Article 113963

[Purchase PDF](#) Article preview

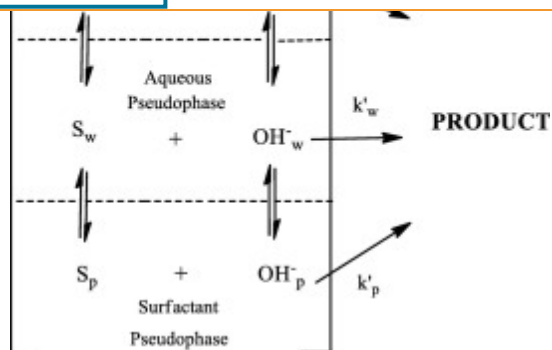
FEEDBACK

Submit your article

Menu



Search in this journal



Research article ○ Abstract only

Influence of hydrogen bond on the mesomorphic behaviour in urethane based liquid crystalline compounds: Experimental and computer simulation study

Burak Korkmaz, Sinem Agtas, Berkay Sütay, Erol Yildirim, ... Yesim Gursel

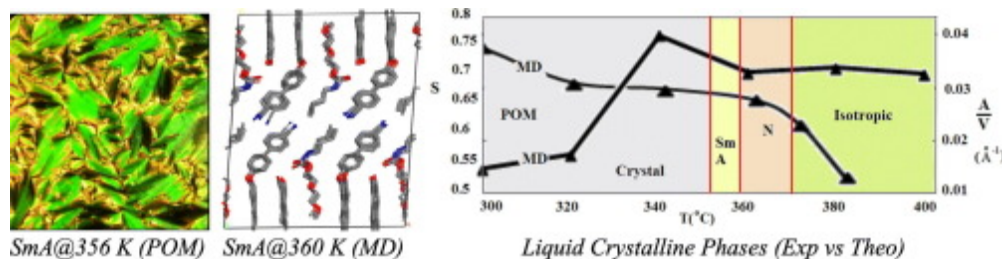
Article 114001

[Purchase PDF](#) Article preview

Abstract

Graphical abstract

Graphical abstract

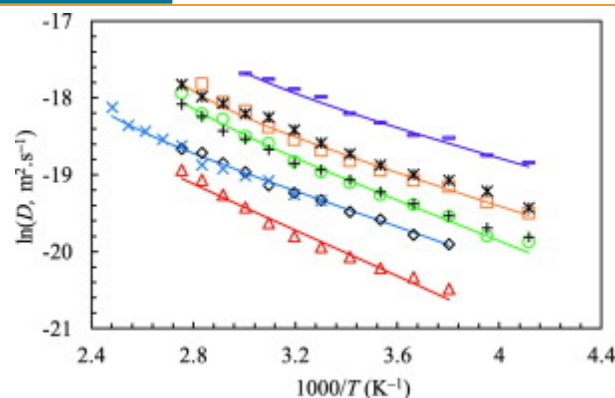


Research article ○ Abstract only

Molecular dynamic simulation and SAFT modeling of the viscosity and self-diffusion coefficient of low global warming potential refrigerants

Wael A. Fouad, Hassan Alasiri

FEEDBACK



Research article ○ Abstract only

Hydrogen sulfide solubility in different ionic liquids: an updated database and intelligent modeling

Mostafa Hosseini, Reza Rahimi, Mojtaba Ghaedi

Article 113984

[Purchase PDF](#) Article preview [Article preview](#)

Abstract

Abstract

Hydrogen sulfide is an acidic, corrosive, toxic, and flammable gas, which is found extensively in the oil and gas industry. For processing of oil and gas and also for the sake of environmental consideration, the sour gas must be removed. This is usually performed through the application of the gas-liquid absorption processes. Ionic liquids are comparatively novel solutions with desirable properties and do not exhibit the disadvantages, which are associated with common amine-based solutions. Their remarkable properties such as negligible vapor pressure, high thermal and electrochemical stabilities, high solubility, and non-flammability make them a good alternative to classical liquid solvents in the field of gas separation and adsorption. Establishing models for accurate estimation of solubility is an appropriate

[Submit your article](#)[Menu](#)[Search in this journal](#)[Purchase PDF](#) [Article preview](#)

Abstract

Abstract

Ionic liquids (ILs) show great potentials for CO₂ capture. In this research, we perform molecular dynamics (MD) simulations to explore bulk and interfacial behaviors of [Bmim][Ac] and [Bmim][BF₄] ILs with and without CO₂, in terms of transport phenomena and thermodynamics aspects. Physiochemical properties of pure ILs are calculated; structural properties such as radial distribution function (RDF) and self-diffusivity of the cations and anions are determined at various conditions. Great agreement is achieved between the experimental and calculated properties. Diffusion coefficients obtained for the cations and anions of the ILs are in the range of 3×10^{-12} to 34×10^{-12} m²/s. The cations have a higher diffusivity than the anions. It is found that the anion has an important effect on CO₂.

[Research article](#) ☐ [Abstract only](#)

Photodegradation of methylene blue and some emerging pharmaceutical micropollutants with an aqueous suspension of WZnO-NH₂@H₃PW₁₂O₄₀ nanocomposite

R. Tayebie, E. Esmaeili, B. Maleki, A. Khoshniat, ... N. Mollania

Article 113928

[Purchase PDF](#) [Article preview](#)

Abstract

Graphical abstract

Graphical abstract

WZnO-NH₂@H₃PW₁₂O₄₀ (WZnO/HPA) nanocomposite is disclosed for the photocatalytic degradation of a range of wastewaters.

[FEEDBACK](#)

[Submit your article](#)[Menu](#)[Search in this journal](#)Research article ☐ Abstract only

Lanthanide-titanium oxo-clusters, new precursors of multifunctional colloids for effective imaging and photodynamic therapy

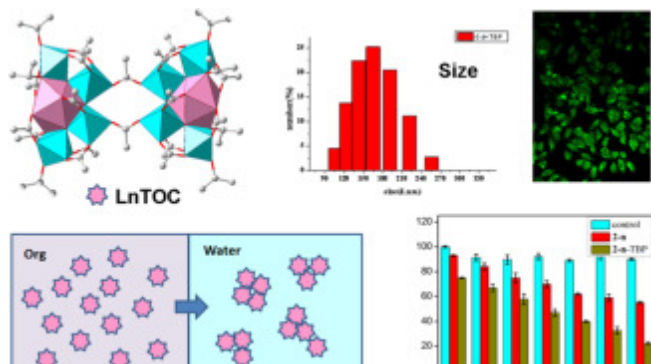
Wen Luo, Xian-Ping Shu, Pei-Yi Liu, Shuai-Kang Yu, ... Jie Dai

Article 113946

[Purchase PDF](#) [Article preview](#)[Abstract](#)[Graphical abstract](#)

Graphical abstract

A convenient method to prepare low-energy light activatable nano PDT materials from lanthanide-titanium oxo-clusters (LnTOCs).

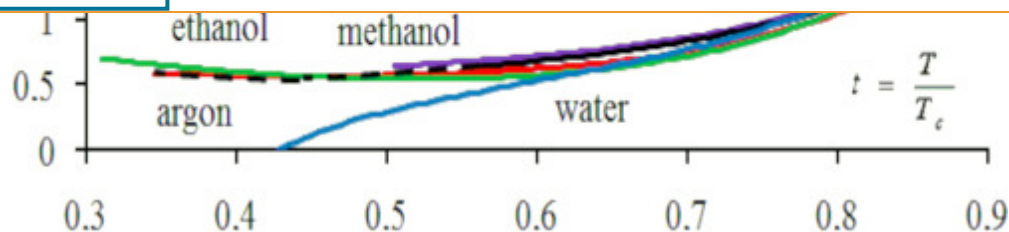
Research article ☐ Abstract only

Similarity degrees and differences of argon, hydrogen sulphide, water, methanol and ethanol on their coexistence curves

Vladimir E. Chechko, Vladimir Ya. Gotsulskiy, Nikolay P. Malomuzh

Article 113941

[Purchase PDF](#) [Article preview](#)[FEEDBACK](#)

[Submit your article](#)[Menu](#)[Search in this journal](#)

Research article ○ Abstract only

A model based on the equality of chemical potentials for describing the liquid-liquid interfaces of water-hydrocarbons up to high pressures

Shahin Khosharay, Parivash Feyzi, Sedigheh Tourang, Farhad Tajfar

Article 113931

[Purchase PDF](#) Article preview [Article preview](#)

Abstract

Abstract

A reliable model was used to describe the interfacial tension, composition, and density of the liquid-liquid interfaces of water-hydrocarbons. The parachor model was combined with the equality of the chemical potential of components at the interface and the bulk liquid. The fugacity coefficient was used for computing chemical potentials. To compute the fugacity coefficients of the components, various types of equations of state (The Valderrama Patel-Teja, cubic plus association, and the simplified Perturbed-Chain Statistical Association Fluid Theory) were utilized. These models were applied to the temperature and the pressure range of (285.65–423) K and (1–3000) bar, respectively. The adjustable parameters of these models were regressed based on the experimental interfacial tensions of (water/hydrocarbon) binary systems

Research article ○ Abstract only

[FEEDBACK](#)

[Submit your article](#)[Menu](#)[Search in this journal](#)[Abstract](#)

Abstract

In this work, a developed adsorption model was brought forward based on the sigmoid model. Under certain conditions, the model is mathematically equivalent to the hyperbolic model, and it has the ability to predict the adsorption equilibrium time and the adsorption mass of the adsorbent per unit mass of adsorbent in equilibrium. The proposed model can be deduced to the empirical model and other forms under certain conditions. The aim of this study is to obtain a mathematically simplified model, provide a probability to predict related parameters and offer mathematical sights into the Langmuir kinetics. The proposed model is verified through experimental study and the results show that it has a prominent agreement with the experimental data. The model can be dedicated to driving the process of dynamic analysis from

Research article ○ Abstract only

Evaluation of thermodynamic parameters via reaction stoichiometry and the corrected Langmuir parameter for sorption of Cu(II) on chitosan and chitosan blended PVA films

Preeti Kulkarni, Varuna Watwe, Gayatri Pathak, Sana Sayyad, Sunil Kulkarni

Article 113962

[Purchase PDF](#) Article preview [^](#)

[Abstract](#)

Abstract

Natural Chitosan (C) and Chitosan blended with Poly vinyl Alcohol (PVA) C + P film was prepared by solution casting method for the sorption of Cu(II) from aqueous solution. The FTIR studies revealed that the amino group of chitosan played key roles in the copper uptake and FE-SEM and EDAX studies confirmed the formation of Cu-amino complex in 1:1 ratio of metal to ligand. The prime objective of present studies is the evaluation of thermodynamic parameters

[FEEDBACK](#)

Journal of Molecular Liquids

Supports *open access*

Submit your article

Menu



Search in this journal

Spectral analysis and DFT investigation of some benzopyran analogues and their self-assemblies with graphene

Jamelah S. Al-Otaibi, Y. Sheena Mary, Y. Shyma Mary, Savaş Kaya, Sultan Erkan

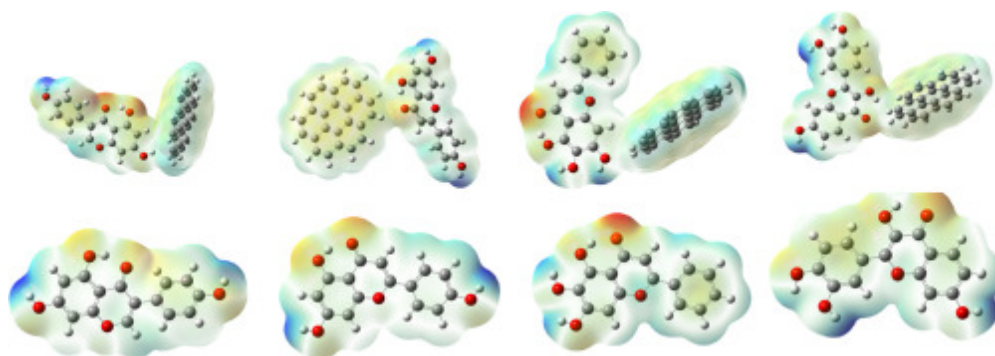
Article 113924

[Purchase PDF](#) Article preview

Abstract

Graphical abstract

Graphical abstract



Research article ○ Abstract only

Solubility, thermodynamic properties, HSP, and molecular interactions of vitamin K₃ in pure solvents

Yi Yu, Fanfan Li, Shanghai Long, Li Xu, Guoji Liu

Article 113945

[Purchase PDF](#) Article preview

Abstract

Abstract

FEEDBACK

Submit your article

Search in this journal

appropriate model to describe solubility of vitamin K₃ in these ten solvents; it provides

Research article ○ Abstract only

Thermodynamic properties of Mg-Pd liquid alloys

A. Dębski, S. Terlicka, W. Gąsior, W. Gierlotka, ... M. Polański

Article 114024

 Purchase PDF Article preview 

Abstract

Abstract

This paper presents the first integral mixing enthalpies of Mg-Pd liquid alloys obtained with the use of a drop calorimeter (Setaram MHTC 96 Line Evo). The measurements for this binary system were carried out at 990 K and 1031 K, up to a maximum Pd content of approximately $x_{\text{Pd}}=0.25$. All obtained values were negative under the tested conditions and the examined concentration range. The experimental data of the liquid Mg-Pd solutions were elaborated by the Redlich-Kister equation.

Research article ☐ Abstract only

Estimation of heat capacities of gases, liquids and solids, and heat capacities of vaporization and of sublimation of organic chemicals at 298.15 K

Michael H. Abraham, William E. Acree

Article 113969

[Purchase PDF](#) [Article preview](#)

Abstract

Graphical abstract

FEEDBACK 

Submit your article

Menu



Search in this journal



Liquid, Cp(liquid)



Solid, Cp(solid)

Research article ○ Abstract only

Enhanced charge carrier conduction and other characteristic parameters of hexagonal plastic columnar phase of a discotic liquid crystalline material due to functionalized gold nanoparticles

Akanksha Khare, Rahul Uttam, Sandeep Kumar, Ravindra Dhar

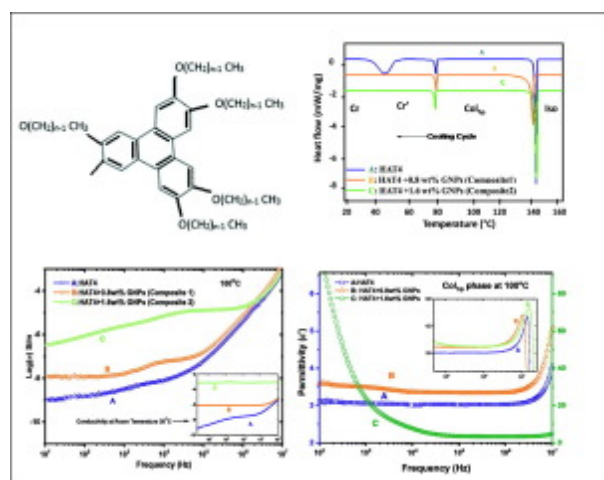
Article 113985

[Purchase PDF](#) Article preview

Abstract

Graphical abstract

Graphical abstract



Research article ○ Abstract only

FEEDBACK

Submit your article

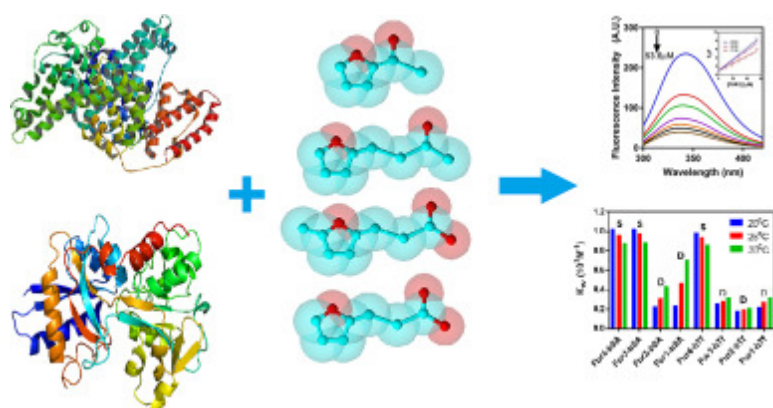
Menu

Search in this journal

Abstract

Graphical abstract

Graphical abstract



Research article ○ Abstract only

Interpretation of hydrogen bonding formation through thermodynamic, spectroscopic and DFT studies between isoamyl alcohol and benzyl alcohol at $T = (293.15 \text{ to } 318.15) \text{ K}$

B. Satheesh, D. Sreenu, M. Chandrasekhar, T. Savitha Jyostna

Article 113942

[Purchase PDF](#) Article preview [Article preview](#)

Abstract

Graphical abstract

Graphical abstract

FEEDBACK

[Submit your article](#)[Menu](#)[Search in this journal](#)

A thermokinetic model for penetrant-induced swelling in polymeric membranes: Water in polybenzimidazole membranes

Mahboubeh Pishnamazi, Azam Marjani, Marieh Pishnamazi, Peyman Pouresmaeel Selakjani, Saeed Shirazian

Article 114000

[Purchase PDF](#)[Article preview](#)

Abstract

Abstract

This paper reports development and validation of a thermokinetic model capable of tracking time-dependent water penetration and the corresponding swelling in polymeric membranes, polybenzimidazoles as case study here. This attempt is highly important as the effect of water in separation performance and properties of membrane is a hot topic to understand the separation mechanism. Specially as humidity in feed gas is common in most of industrial gas separation processes noting that water penetration can cause swelling which may result in variation in mass transport and mechanical deformation in form of thickness change. We compared model calculation to relevant reported data showing robustness of developed thermokinetic model.

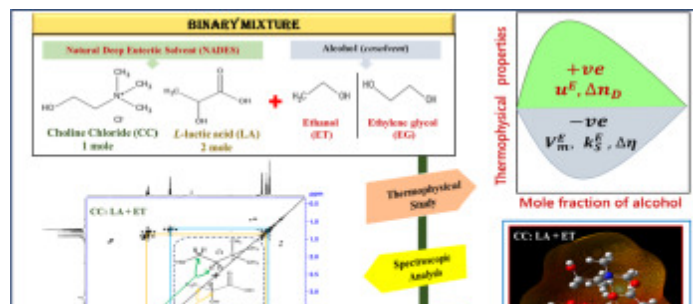
Research article ○ Abstract only

Acumen into the effect of alcohols on choline chloride: L-lactic acid-based natural deep eutectic solvent (NADES): A spectral investigation unified with theoretical and thermophysical characterization

Anil Kumar Jangir, Harsh Mandviwala, Paras Patel, Sangita Sharma, Ketan Kuperkar

Article 113923

[Purchase PDF](#)[Article preview](#) [FEEDBACK](#)



Research article ○ Abstract only

Effect of titanium oxide nanoparticles on the dielectric properties and ionic conductivity of a new smectic bis-imidazolium salt with dodecyl sulfate anion and cyanobiphenyl mesogenic groups

Constantin Paul Ganea, Viorel Cîrcu, Doina Manaila-Maximean

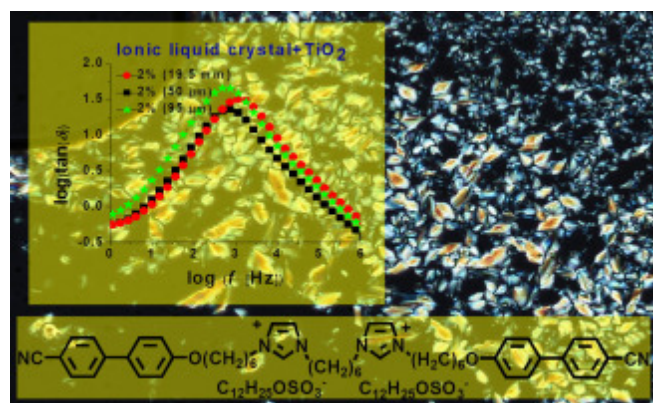
Article 113939

[Purchase PDF](#) [Article preview](#)

Abstract

Graphical abstract

Graphical abstract

Research article ☐ Abstract only

FEEDBACK 

[Submit your article](#)[Menu](#)[Search in this journal](#)[Abstract](#)

Abstract

The solvent phase composed of tetraoctyl diglycolamide (TODGA) in *n*-dodecane (*n*-DD) undergoes the undesirable organic phase splitting during the solvent extraction of trivalent actinides and lanthanides from nitric acid medium. To overcome this limitation a neutral extractant namely the *N,N*-dioctyl hydroxyacetamide (DOHyA), which was half the molecule of TODGA, has been added to the solvent phase and evaluated for the extraction of Nd(III) from nitric acid medium. Since the reverse micellar aggregates of the extracted species in the organic phase was responsible for organic phase splitting, the aggregation behaviour of the organic phase was probed by dynamic light scattering (DLS) technique. The results have been compared with the individual solvent systems namely DOHyA/*n*-DD and TODGA/*n*-DD. The

Research article ○ Abstract only

Investigation of thermophysical properties of aqueous magnesium ferrite nanofluids

R. Kirithiga, J. Hemalatha

Article 113944

[Purchase PDF](#) Article preview [Article preview](#)

[Abstract](#)[Graphical abstract](#)

Graphical abstract

[FEEDBACK](#)

[Submit your article](#)[Menu](#)[Search in this journal](#)

extracted by aqueous two-phase systems PEG/citrate

Lígia Maria Gonçalves Fernandes, Márcia Nieves Carneiro-da-Cunha, Jônatas de Carvalho Silva, Ana Lúcia Figueiredo Porto, Tatiana Souza Porto

Article 113957

[Purchase PDF](#) [Article preview](#)

Abstract

Abstract

A novel *Aspergillus heteromorphus* URM 0269 protease (EC 3.4.21) was extracted by aqueous two-phase systems PEG/citrate (ATPS). Extraction was performed by factorial design 2^4 for analyzing the independent variable effects named PEG molar mass (M_{PEG}), PEG concentration (C_{PEG}), sodium citrate concentration (C_{CTT}) and pH. Afterwards, extracted protease was characterized in terms of kinetic and thermodynamic parameters. Protease partitioned preferentially for the PEG rich phase displaying the highest purification factor of 7.83 with a 157.53% yielded. Despite the enzyme acted optimally at 50 °C and pH 8.0, it was more stable in lower temperatures (10–40 °C) and pH conditions (5.0–10.0). The kinetic parameters of activation for casein hydrolysis revealed higher affinity by casein ($K_m = 2.8 \text{ mg/mL}$) with maximum catalysis

[Research article](#) [Abstract only](#)

Photocatalytic hydrogel layer supported on alkali modified straw fibers for ciprofloxacin removal from water

Xiaoli Huang, Song Wu, Shizhan Tang, Li Huang, ... Qi Hu

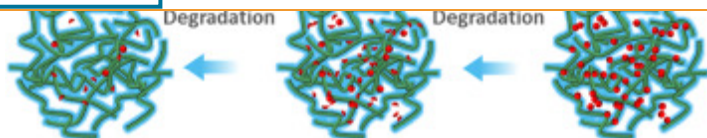
Article 113961

[Purchase PDF](#) [Article preview](#)

Abstract

Graphical abstract

[FEEDBACK](#)

[Submit your article](#)[Menu](#)[Search in this journal](#)[Research article](#) ☐ [Abstract only](#)

Structure-relation properties of N-substituted phenothiazines in solution and solid state: Photophysical, photostability and aggregation-induced emission studies

Ana Clara B. Rodrigues, João Pina, J. Sérgio Seixas de Melo

Article 113966

[Purchase PDF](#) [Article preview](#)

Abstract

Abstract

Five N-substituted phenothiazines (with different alkyl and aryl groups) were investigated aiming to rationalize the influence of the substitution in the photooxidation processes and in the aggregation induced emission (AIE) properties of these compounds. A comprehensive spectroscopic and photophysical investigation in solution (diluted in solutions of methylcyclohexane, MCH, tetrahydrofuran, THF, and in THF: water mixtures aiming to promote aggregation) and in the solid state (powder and films), with the characterization of all the excited state deactivation routes with the determination of quantum yields (fluorescence, phosphorescence and singlet oxygen sensitization), lifetimes and rate constants, was performed. Room temperature phosphorescence in the solid state was observed for the methyl

[Research article](#) ☐ [Abstract only](#)

Insight into the solubility and solution thermodynamics of fosfomycin phenylethylamine in water and ethanol for its cooling crystallization

[FEEDBACK](#)

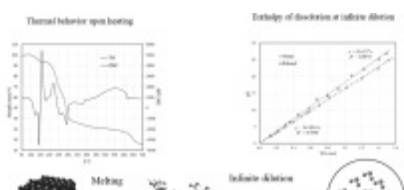
Menu



Search in this journal

Graphical abstract

Fosfomycin phenylethylamine crystalline was characterized by using thermogravimetry and differential scanning calorimetry and its solubility in ethanol and water was systematically measured. An integrated approach by van't Hoff plot, enthalpy-entropy compensation analysis and solution calorimetry was proposed to interpret the non-ideal solubility behavior in both solvents.



Research article ○ Abstract only

Fluorescent detection of Al(III) and CN^- in solid and aqueous phases and their recognition in biological samples

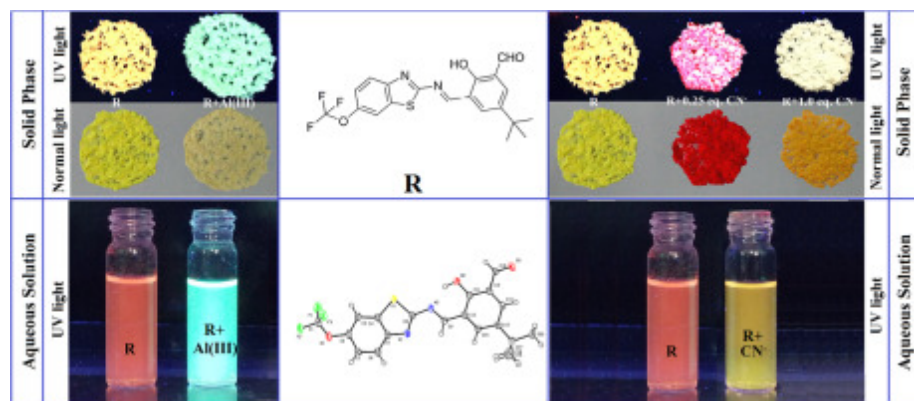
P. Saravana Kumar, S. Ciattini, C. Laura, Kuppanagounder P. Elango

Article 113970

[Purchase PDF](#) Article preview

Abstract Graphical abstract

Graphical abstract



FEEDBACK

[Submit your article](#)[Menu](#)[Search in this journal](#)

Article 113971

[Purchase PDF](#)[Article preview](#)

Abstract

Abstract

In this paper, conductivity and viscosity of 1-alkyl-3-methylimidazolium tricyanomethanide series $[\text{C}_n\text{C}_1\text{im}][\text{TCM}]$, where $n=2, 4, 6$, and 8 were measured and analyzed in the broad temperature range covering supercooled and normal liquid states at ambient pressure. The density at ambient pressure up to 363.15 K was also investigated. From these experimental data, the Walden plots for the studied ionic liquids were obtained and dependencies for all tested samples lie below the reference line for fully dissociated $0.01\text{ mol}\cdot\text{dm}^{-3}\text{ KCl}$. The temperature dependence of viscosity revealed clear crossover from one Vogel–Fulcher–Tamman behavior to another at some intermediate temperature that increases with the alkyl chain length of the cation and we discovered that all examined ILs are fragile glass formers. Additionally, the high-

Research article ○ Abstract only

An experimental-coupled empirical investigation on the corrosion inhibitory action of 7-alkyl-8-Hydroxyquinolines on C35E steel in HCl electrolyte

M. El Faydy, F. Benhiba, A. Berisha, Y. Kerroum, ... A. Zarrouk

Article 113973

[Purchase PDF](#)[Article preview](#)

Abstract

Abstract

Two 8-Hydroxyquinoline-based piperazine, 7-((4-(4-chloro phenyl)piperazin-1-yl) methyl) quinolin-8-ol (CPQ) and 7-((4-methyl piperazin-1-yl) methyl)quinolin-8-ol (MPQ) were

[FEEDBACK](#)

[Submit your article](#)[Menu](#)[Search in this journal](#)[Research article](#) ○ [Abstract only](#)

Thermodynamic properties of liquid Mg—Pt alloys determined by the calorimetric method

S. Terlicka, A. Dębski, W. Gąsior, W. Gierlotka, ... M. Polański

Article 113976

[Purchase PDF](#) [Article preview](#)

Abstract

Abstract

Pioneering thermodynamic measurements of Mg—Pt system are presented. The integral enthalpies of liquid binary alloys were determined using a drop calorimetric method. The obtained results in three independent series were negative in the entire measured concentration range at 1031 K. The studied integral molar mixing enthalpies were compared with the predicted mixing enthalpies based on Miedema's model. The highest difference between the data obtained experimentally and those predicted by the Miedema's model was found to be 3 kJ/mol for $x_{\text{Pt}} = 0.19$. Experimental values of liquid Mg—Pt solutions were also elaborated with the use of Redlich-Kister polynomial. A very good agreement between measurement data and those calculated by the Redlich-Kister was found

[Research article](#) ○ [Abstract only](#)

Unraveling thermodynamic and conformational correlations in action of osmolytes on hen egg white lysozyme

Rajeshree Amit Shinde, Ritutama Ghosh, Pooja Prasanthan, Nand Kishore

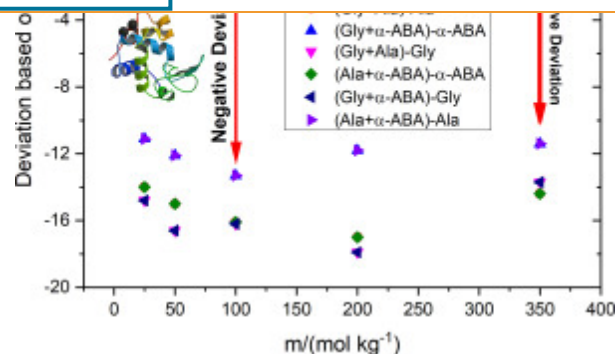
Article 113996

[Purchase PDF](#) [Article preview](#)[FEEDBACK](#)

Menu



Search in this journal



Research article ○ Abstract only

Microextraction and gas chromatography–flame ionization determination of five antiepileptic drugs in biological samples using amino acid-based deep eutectic ionic liquids

Amir Ismailzadeh, Mahboubeh Masrournia, Zarrin Es'haghi, Mohammad Reza Bozorgmehr

Article 113979

[Purchase PDF](#) Article preview

Abstract

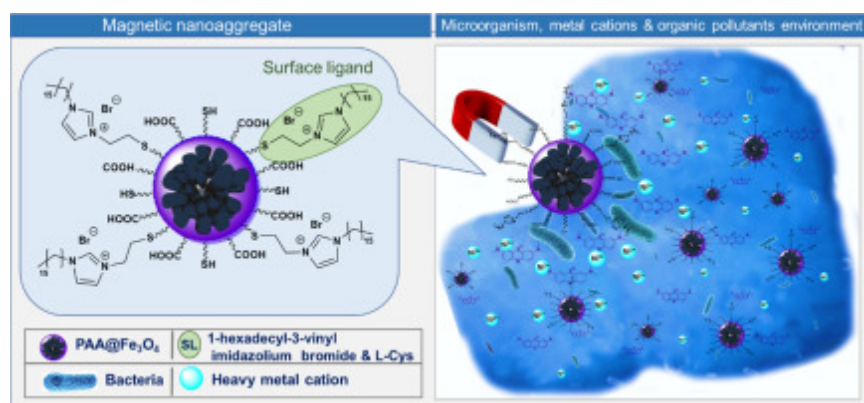
Abstract

This study investigated the use of amino acid-based deep eutectic solvents (AADESs) in the ultrasound assisted reverse-phase emulsification microextraction (UARPEME) of five antiepileptic drugs (AEDs) from biological samples. The extraction was performed by dispersing the AADES into the sample solution using ultrasonic irradiation. After completing extraction, the sample solution was centrifuged. Then, the pre-concentrated AEDs in the AADES (upper phase) were derivatized by adding phenyltrimethylammonium hydroxide solution to it. The derivatized analytes were then eluted with n-hexane and it was injected directly into the gas chromatography–flame ionization detection (GC–FID) system to determine target analytes after the methylation reaction inside the injection chamber. The

FEEDBACK

[Submit your article](#)[Menu](#)[Search in this journal](#)[Abstract](#)[Graphical abstract](#)

Graphical abstract

Research article ☐ Abstract only

Soft nanocarriers for new poorly soluble conjugate of pteridine and benzimidazole: Synthesis and cytotoxic activity against tumor cells

Alla B. Mirgorodskaya, Darya A. Kuznetsova, Rushana A. Kushnazarova, Dinar R. Gabdrakhmanov, ...
Lucia Y. Zakharova

Article 114007

[Purchase PDF](#) [Article preview](#)[Abstract](#)[Graphical abstract](#)

Graphical abstract

[FEEDBACK](#)

[Submit your article](#)[Menu](#)[Search in this journal](#)

Research article ○ Abstract only

Construction of zwitterionic surfactant-stabilized hydrophobic ionic liquid-based bicontinuous microemulsion and microstructure-dependent activity of solubilized lipase

Rongrong Wang, Wei Jin, Xirong Huang

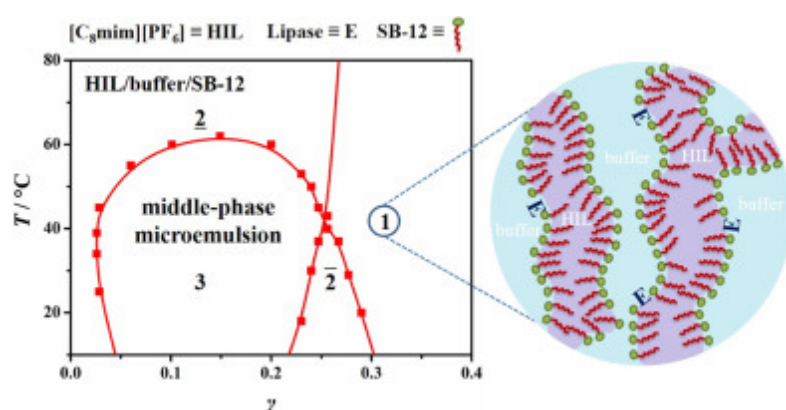
Article 114011

[Purchase PDF](#) Article preview

Abstract

Graphical abstract

Graphical abstract



Research article ○ Abstract only

Relevance of π -stacking in tuning the neighboring structural pattern of soft nano-aggregates

Gulmi Chakraborty, Soumik Bardhan, Soumen Ghosh, Swapan K. Saha

Article 114013

[Purchase PDF](#) Article preview

Abstract

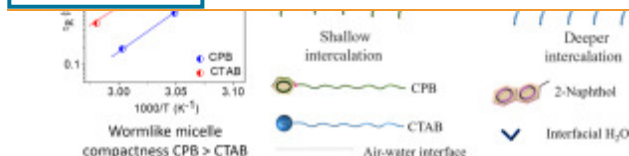
Graphical abstract

[FEEDBACK](#)

Menu



Search in this journal



Research article ○ Abstract only

Evaluation of ionic liquids as electrolytes for vanadium redox flow batteries

L. Bahadori, R. Boyd, A. Warrington, M.S. Shafeeyan, P. Nockemann

Article 114017

[Purchase PDF](#) Article preview

Abstract

Abstract

Non-aqueous redox flow batteries (NARFBs) are promising electrochemical energy storage devices due to their wide electrochemical potential windows, generally >2 V of organic solvents. This study aims to investigate the suitability of ionic liquids (ILs) as electrolytes for NARFBs containing a vanadium metal complex. The electrochemistry of a single-component NARFBs employing vanadium (III) acetylacetonate ($V(acac)_3$) was studied in 1-butyl-3-methylimidazolium bis(trifluoromethylsulfonyl)imide, $[C_4mim][NTF_2]$, and 1-butyl-1-methylpyrrolidinium bis(trifluoromethanesulfonyl)imide, $[C_4mpyr][NTF_2]$, electrolytes. The electrochemical kinetics of the anodic and cathodic reactions was measured using cyclic voltammetry. The V^{II}/V^{III} and V^{III}/V^{IV} couples were quasi-reversible and together yielded a cell

Research article ○ Abstract only

Viscosity and isobaric specific heat capacity of alumina nanoparticle enhanced ionic liquids: An experimental approach

Elena Ionela Cherecheș, Jose I. Prado, Constanta Ibanescu, Maricel Danu, ... Luis Lugo

FEEDBACK

[Submit your article](#)[Menu](#)[Search in this journal](#)

Temperature and loading dependences on the rheological behavior and isobaric specific heat capacity of several suspensions of alumina nanoparticles in a binary mixture of $[\text{C}_2\text{mim}][\text{CH}_3\text{SO}_3]$ ionic liquid and water were experimentally determined to assess its potential condition of enhanced heat transfer fluids. Rheological tests show a clear Newtonian behavior for the base fluid and the NEILs with lower Al_2O_3 concentrations while higher amounts of alumina nanoparticles entail non-Newtonian fluids and increase in viscosity up to 78%. The heating-cooling viscosity tests reveal that no significant viscosity hysteresis occur and VFT equation adequately describe the temperature dependence. Isobaric specific heat capacities decrease ($<10\%$) with nanoparticle mass fraction and increase ($<10\%$) with temperature. The

[Research article](#) ☐ [Abstract only](#)

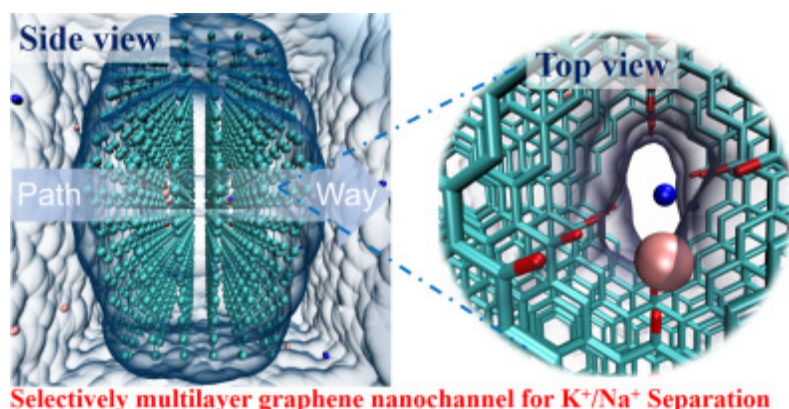
Voltage-gated multilayer graphene nanochannel for K^+/Na^+ separation: A molecular dynamics study

Ke Gong, Timing Fang, Ting Wan, Youguo Yan, ... Jun Zhang

Article 114025

[Purchase PDF](#) [Article preview](#)[Abstract](#)[Graphical abstract](#)

Graphical abstract

[FEEDBACK](#)

[Submit your article](#)[Menu](#)[Search in this journal](#)[Purchase PDF](#)[Article preview](#)

Abstract

Abstract

We investigate in this paper, via molecular dynamics simulations, the composition dependent solution structures in the binary mixtures composed of the ionic liquid (IL), 1-butyl-3methylimidazolium hexafluorophosphate, ([BMIM] [PF₆]), and three different co-solvents of comparable sizes but with differing polarities. These cosolvents are acetonitrile (dipolar), 1,4-dioxane (quadrupolar) and hexane (non-polar). Five different IL mole fractions for the binary mixtures ($F_{IL} = 0.90, 0.75, 0.50, 0.25, 0.10$) along with the neat solvents have been studied. The cosolvent polarity and concentration dependencies have been assessed through the examination of the composition dependent spatial and radial distribution functions, coordination numbers and the Voronoi polyhedra analyses. The solution structure is found to

[Research article](#) ☐ [Abstract only](#)

Aqueous solubilization and extraction of curcumin enhanced by imidazolium, quaternary ammonium, and tropine ionic liquids, and insight of ionic liquids-curcumin interaction

Jinghang Li, Zhixia Wang, Shun Yao, Hang Song

Article 113906

[Purchase PDF](#)[Article preview](#) [Abstract](#)[Graphical abstract](#)

Graphical abstract

[FEEDBACK](#)

[Submit your article](#)[Menu](#)[Search in this journal](#)Research article [Open access](#)

Hydrolysis of eutectic compositions in the $\text{ZnCl}_2\text{:KCl:NaCl}$ ternary system and effect of adding ZnO

Sepideh Niazi, Espen Olsen, Heidi S. Nygård

Article 114069

[Download PDF](#) [Article preview](#)

Abstract

Abstract

Molten salt systems have been considered as proper liquefiers, solvents and transfer media due to their transport and thermodynamic properties. Employing molten salts to liquify biomass could be performed to make it pumpable and transfer it more easily through thermochemical conversion processes to e.g. bio-oil. The first challenge for this application is to find a salt with relatively low melting point. It needs to be low enough to avoid producing ash or char and at the same time high enough to liquify biomass. The selected molten salt requires high thermal stability to avoid salt decomposition at high temperatures and make salt recycling possible. Another challenge is minimising the hydrolysis rate of the molten salt in contact with water molecules originated from the biomass because this can lead to undesired formation of highly

Research article ☐ Abstract only

A facile approach to synthesis of cobalt ferrite nanoparticles with a uniform ultrathin layer of silicon carbide for organic dye removal

T. Muthukumaran, John Philip

Article 114110

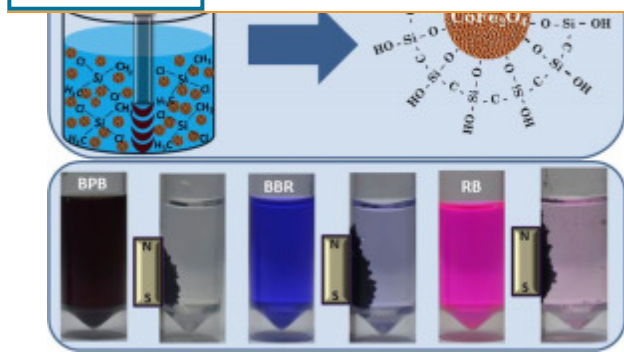
[Purchase PDF](#) [Article preview](#)[FEEDBACK](#)

Submit your article

Menu



Search in this journal

Research article ☐ Abstract only

Fabrication of graphene nanosheets decorated by nitrogen-doped ZnO nanoparticles with enhanced visible photocatalytic activity for the degradation of Methylene Blue dye

M. Suresh, A. Sivasamy

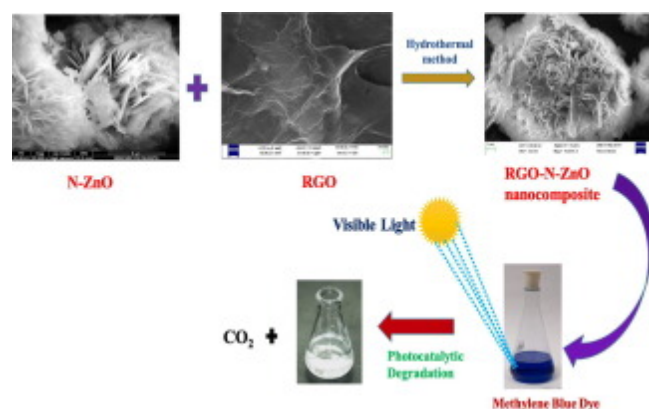
Article 114112

[Purchase PDF](#)
[Article preview](#)

Abstract

Graphical abstract

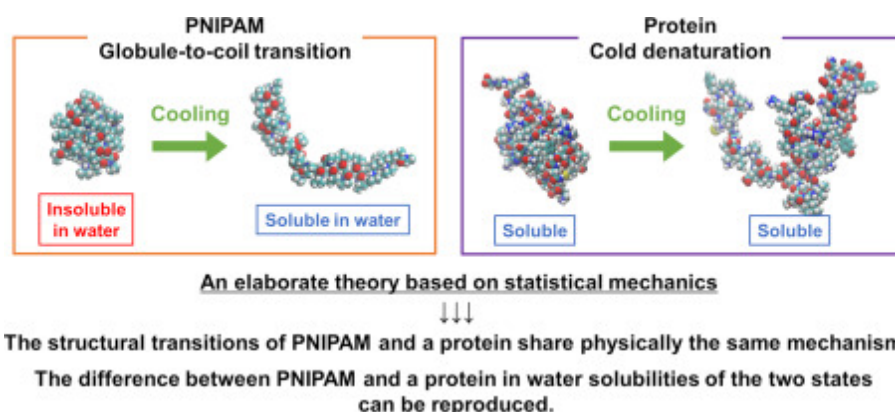
Graphical abstract

Research article ☐ Abstract only

FEEDBACK

[Submit your article](#)[Menu](#)[Search in this journal](#)[Abstract](#)[Graphical abstract](#)

Graphical abstract



Research article ○ Abstract only

Determination of a critical separation concentration for associative polymers in porous media based on quantification of dilute and semi-dilute concentration regimes

Richard O. Afolabi, Gbenga F. Oluymi, Simon Officer, Johnson O. Ugwu

Article 114142

[Purchase PDF](#) [Article preview](#)[Abstract](#)

Abstract

Hydrophobic interactions are an inherent property of associative polymers which results in the formation of molecular aggregates. The loss of hydrophobic interactions under reservoir conditions have been reported, and this results in increased fluid – rock interaction effect such as adsorption. However, existing adsorption studies only reports the interaction of individual molecules with rock surface without taking into account mechanically retained molecular aggregates in narrow pores. The implication of this is a reduction in associative

[FEEDBACK](#)

Journal of Molecular Liquids

Supports *open access*

Submit your article

Menu

 Search in this journal

Andrei V. Yermalayeu, Mikhail A. Varfolomeev, Sergey P. Verevkin

Article 114150

 [Purchase PDF](#) Article preview 

Abstract **Graphical abstract**

Graphical abstract



Research article ○ Abstract only

Fluoride-free electropolymerization of 3-aminophenylboronic acid in room temperature ionic liquids without exogenous protons

Feixue Zou, Yaqiu Kong, Bo Cui

Article 114141

 [Purchase PDF](#) Article preview 

Abstract **Graphical abstract**

Graphical abstract

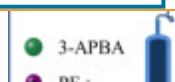
FEEDBACK 

Submit your article

Menu



Search in this journal

Research article ☐ Abstract only

Constructing hydrangea-like hierarchical zinc-zirconium oxide microspheres for accelerating fluoride elimination

Ming Gao, Wei Wang, Mengbo Cao, Hongbing Yang, Yongsheng Li

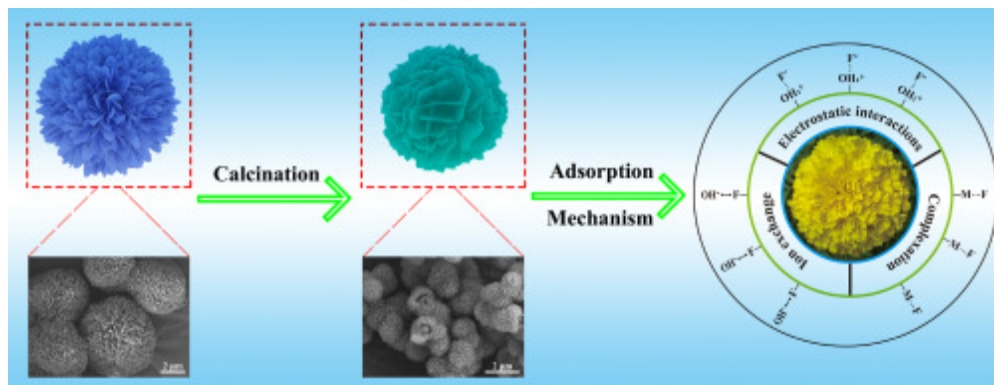
Article 114133

[Purchase PDF](#) Article preview

Abstract

Graphical abstract

Graphical abstract

Research article ☐ Abstract only

NMR study of the influence and interplay of water, HCl and LiCl with the extraction agent Aliquat 336 dissolved in toluene

Hans Vigeland Lerum, Niels Højmark Andersen, Dag Øistein Eriksen, Eddy Walther Hansen, Jon Petter Omtvedt

Article 114160

FEEDBACK

with aqueous solutions containing LiCl or HCl. After mixing, the organic phase was separated from the aqueous phase and analysed using NMR and acid–base titration. The different proton species HCl, H₂O and H₃O⁺ present in the aqueous phase are normally not distinguishable using NMR due to fast exchange conditions (on the NMR time scale) and therefore they give rise to mainly one single peak in the proton spectrum. The chemical shift of this single ‘composite’ peak is affected by the relative distribution of the various proton species present in the aqueous solution and is made use of in this work. For instance, ratio of molecular hydrochloric acid (HCl) and dissociated acid (H₃O⁺·Cl[−]) was found to be between 0.966 and

Research article ☐ Abstract only

Arsenic selective adsorption using a nanomagnetic ion imprinted polymer: Optimization, equilibrium, and regeneration studies

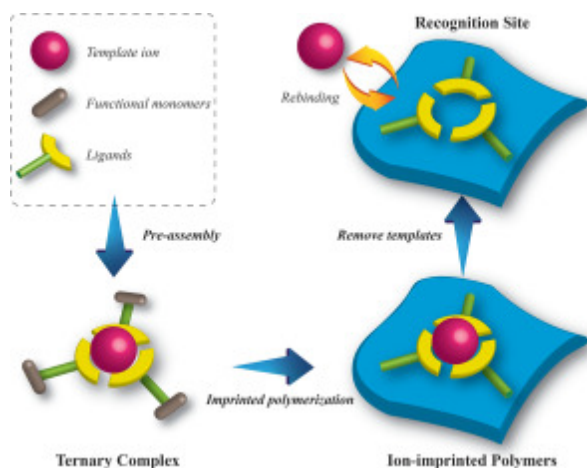
Mohsen Sadani, Tayebah Rasolevandi, Hossein Azarpira, Amir Hossein Mahvi, ... Ali Atamaleki
Article 114246

 [Purchase PDF](#) Article preview 

Abstract

Graphical abstract

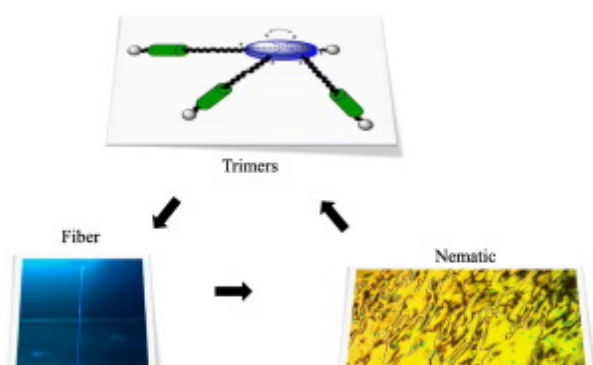
Graphical abstract



[Submit your article](#)[Menu](#)[Search in this journal](#)[Purchase PDF](#) [Article preview](#)[Abstract](#)[Graphical abstract](#)

Graphical abstract

The first examples of low symmetry trimers and these materials provide access to unique low molar mass nematics capable of forming freely suspended fibers.

[Research article](#) ☐ [Abstract only](#)

New effects of TiO_2 nanotube/ $\text{g-C}_3\text{N}_4$ hybrids on the corrosion protection performance of epoxy coatings

Sepideh Pourhashem, Jizhou Duan, Fang Guan, Nan Wang, ... Baorong Hou

Article 114214

[Purchase PDF](#) [Article preview](#)[Abstract](#)[Graphical abstract](#)

Graphical abstract

[FEEDBACK](#)

[Submit your article](#)[Menu](#)[Search in this journal](#)[Research article](#) ○ [Abstract only](#)

Influence of the hydrophilic moiety of polymeric surfactant on their surface activity and physical stability of pesticide suspension concentrate

Shupeng Zhang, Xiaodong Yang, Zhenbei Tu, Wendong Hua, ... Tianrui Ren

Article 114136

[Purchase PDF](#) [Article preview](#)

Abstract

Abstract

Polymeric surfactant has explored as an efficient dispersant for improving the physical stability of pesticide suspension concentrate. However, the influence of the hydrophilic monomer on the surface-active property of polymeric surfactant and its application performance in pesticide formulation is rare investigated. Herein, three kinds of random polymers were designed and synthesized via polymerization reaction of styrene (St), methacrylic acid (MAA) with 2-hydroxyethyl acrylate (HEA), 2-hydroxypropyl acrylate (HPA) and vinyl sulfonate sodium (VS), respectively. A series of surface-active parameters, including critical aggregation concentration (CMC), saturation surface excess concentration (Γ_{\max}), minimum area per molecule (A_{\min}) and standard Gibbs free energy ΔG^0 values were obtained from surface tension measurement

Journal of Molecular Liquids

Supports *open access*

Submit your article

Menu



Search in this journal

ELSEVIER

FEEDBACK 

See discussions, stats, and author profiles for this publication at: <https://www.researchgate.net/publication/343379587>

Comparing natural and synthetic polymeric nanofluids in a mid-permeability sandstone reservoir condition

Article in *Journal of Molecular Liquids* · August 2020

DOI: 10.1016/j.molliq.2020.113947

CITATIONS

7

READS

149

10 authors, including:



Agi Augustine

Universiti Teknologi Malaysia

71 PUBLICATIONS 949 CITATIONS

[SEE PROFILE](#)



Radzuan Junin

Universiti Teknologi Malaysia

176 PUBLICATIONS 2,430 CITATIONS

[SEE PROFILE](#)



Afeez Olayinka Gbadamosi

Universiti Teknologi Malaysia

62 PUBLICATIONS 1,026 CITATIONS

[SEE PROFILE](#)



Mohammad A. Manan

Universiti Teknologi Malaysia

50 PUBLICATIONS 1,194 CITATIONS

[SEE PROFILE](#)

Some of the authors of this publication are also working on these related projects:



A study of biodiesel from waste cooking oil catalyzed by Sarawak novel ostrich-eggshell based catalyst (2016 - 2019) (now looking for a Graduate Research Assistant (GRA)) [View project](#)



Waxy crude oils flow behavior [View project](#)



Comparing natural and synthetic polymeric nanofluids in a mid-permeability sandstone reservoir condition

Augustine Agi^{a,b}, Radzuan Junin^{a,b,*}, Afeez Gbadamosi^{a,c}, Muhammad Manan^a, Mohd Zaidi Jaafar^{a,b,*}, Mohammed Omar Abdullah^d, Agus Arsad^b, Nur Bashirah Azli^a, Muslim Abdurrahman^e, Faruk Yakasai^{a,f}

^a Department of Petroleum Engineering, School of Chemical and Energy Engineering, Faculty of Engineering, Universiti Teknologi Malaysia, 81310 Johor Bahru, Malaysia

^b Drilling and Production Enhanced Research Group, UTM MPRC-Institute for Oil and Gas, Universiti Teknologi Malaysia, 81310 Johor Bahru, Malaysia

^c Department of Chemical and Petroleum Engineering, College of Engineering, Afe Babalola University, PMB 5454 Ado-Ekiti, Nigeria

^d Department of Chemical Engineering and Energy Sustainability, Faculty of Engineering, Universiti Malaysia Sarawak, Kota Samarahan, Sarawak, Malaysia

^e Department of Petroleum Engineering, Universitas Islam Riau, Jl. Kaharudin Nasution, No. 113 KM 11, Perhentian Marpoyan, Pekanbaru, 28284, Riau, Indonesia

^f Department of Chemical and Petroleum Engineering, Faculty of Engineering, Bayero University, Kano PMB3011, Nigeria

ARTICLE INFO

Article history:

Received 12 April 2020

Received in revised form 5 July 2020

Accepted 28 July 2020

Available online 1 August 2020

Keywords:

Biopolymer

Polymeric nanofluids

Starch nanoparticles

Thermal degradation

EOR

ABSTRACT

Biopolymeric nanofluids have been proposed as an eco-friendly substitute to synthetic polymeric nanofluids to cut cost and environmental effect. However, previous studies on the use of biopolymeric nanofluids to enhance oil recovery focused only on adsorption and fluid injectivity at ambient condition. In this study, the thermal degradation of crystalline starch nanofluid (CSNF) at reservoir condition was investigated and compared with silica and aluminium oxide polymeric nanofluids, SiO₂PNF and Al₂O₃PNF respectively. The thermal degradation of the polymeric nanofluids was investigated using Brookfield RST rheometer. Moreover, interfacial tension (IFT) properties and wettability alteration efficiency of the polymeric nanofluids were determined using Easy Dyne KRUS tensiometer and sessile drop technique, respectively. Finally, the oil displacement ability of the polymeric nanofluids at typical reservoir condition was studied using Fars EOR technologies high-pressure high-temperature apparatus. Experimental result shows that the viscosities of SiO₂PNF and Al₂O₃PNF decreased with increase in temperature, whereas the viscosity of CSNF increased with temperature. Besides, CSNF exhibited a significant decrease in IFT at all conditions investigated while IFT results of SiO₂PNF and Al₂O₃PNF showed a non-monotonic trend with increase in temperature. Moreover, CSNF showed better potential to alter wettability at all conditions. The microscopic image of the emulsion generated shows stability of the emulsion over a long period and confirmed the ability of CSNF to withstand high temperature degradation compared to SiO₂PNF and Al₂O₃PNF. Finally, it was observed that the mobility ratio of water flooding approaches unity faster than that of SiO₂PNF, Al₂O₃PNF and CSNF, respectively. It can be concluded from this study that 13–23% incremental oil recovery can be achieved with the use of polymeric nanofluids.

© 2020 Published by Elsevier B.V.

1. Introduction

The low production from existing reservoirs and less discoveries of new fields has posed a real problem to the oil and gas industries. About 50–70% original oil in place (OOIP) are still trapped in the reservoir after initial recovery and water flooding [1]. Enhanced oil recovery (EOR) methods are one of the viable options that can reduce the gap between demand and supply. EOR processes are used to improve the productivity of the fields which aims to recover the oil left in the reservoirs.

Over the years numerous EOR methods such as gas, thermal and chemical (alkali, surfactants, and polymers) have been used to overcome the low oil sweep efficiency [2]. Chemical EOR (CEOR) technique is deemed highly favourable due to its better proficiency, reasonable capital cost, practical and financial possibilities. EOR chemicals such as alkali and surfactants can reduce interfacial tension (IFT) by altering rock/fluid interface in the reservoir. They can also alter wettability between oil-water (O/W) interface [3]. Polymer flooding is the widely applied CEOR technique to increase viscosity and control mobility. Field results have shown that it can recover up to 5–30% OOIP [4].

Hydrolysed polyacrylamide (HPAM) is a widely used polymer in flooding, because of inexpensive handling cost, relatively resistant to bacterial attack, high solubility in water and high ability to reduce permeability of water [5,6]. However, with variation in crude oil properties and harsh environmental conditions of the reservoir, current chemical

* Corresponding authors at: Department of Petroleum Engineering, School of Chemical and Energy Engineering, Faculty of Engineering, Universiti Teknologi Malaysia, 81310 Johor Bahru, Malaysia.

E-mail addresses: r-radzuan@utm.my (R. Junin), mzaidi@utm.my (M.Z. Jaafar).

flooding materials have limitations such as degradation and precipitation. Therefore, various studies are being carried out to improve the limitations of polymers such as HPAM against high temperature and high salinity reservoir conditions. More recently, researchers have reported the use of nanofluid in CEOR process. Nanofluid which is the synergy of base fluid with nanoparticles has the advantages of being more tolerant to high salinity, high temperature, longer stability, less plugging and retention in highly permeable reservoir [7].

The recent trend in nanotechnology has focused on incorporating polymers with nanoparticles to produce fluids with distinct characteristics from the polymers and nanoparticles [8]. Various studies have reported the use of silica (SiO_2) [9–11]; titanium dioxide (TiO_2) [12]; graphene oxide (GO) [13]; and aluminium oxide (Al_2O_3) [5] nanoparticles to improve the viscosity, degradation, salinity, and viscoelastic properties of HPAM. They reported that the presence of nanoparticles significantly improved the properties of HPAM against environmental factors. Despite the extensive investigation from previous research for EOR application, there are still some challenges on its field application owing to cost, transport and retention in reservoir might pose huge environmental problems [14,15]. Nanoparticles from renewable materials have been sought after to replace inorganic and metallic nanoparticles. The large-scale availability of starches, cellulose and fibres that are known to have long chain polysaccharides to withstand harsh reservoir conditions and their broad applicability has attracted researchers. Starch nanoparticles have found success in pharmaceutical, confectionary, cosmetics, food industry and more importantly EOR.

Wei et al. [15] and Molnes et al. [16] have reported the use of cellulose nanoparticles and crystalline cellulose nanoparticles respectively as displacement fluids in EOR. The cellulose nanofluid were stable and well dispersed in 2.0 wt% of electrolyte and the oil displacement in a micromodel showed that the cellulose nanofluid enhanced the sweep efficiency and decreased residual oil saturation [15]. The flooding experiments show that the cellulose nanocrystals have good injectivity and the rheological properties show stable and long propagation through the core [16]. However, in the study by Molnes et al. [16], sandstone cores were used whereas Wei et al. [15] reported the use of sand-pack and a micromodel in their study. Sand-packs and micromodels are only representative of reservoir cores, as they cannot provide the real heterogeneity of a reservoir. Furthermore, while the procedure for preparing micromodel, glass beads and sand-packs is proper, it does not consider the likelihood of fluid propagation through the sidewalls. Fines movement and fluid channelling through sidewalls occur in a sand-pack/micromodel flooding test and are not considered, despite having significant influence on the flooding result. Overall, both studies failed to consider the effect of temperature in the flooding process, the thermal degradation of the biopolymeric nanofluids in porous media and the mechanisms of EOR.

For us to come to a logical conclusion in the search for a high performance EOR chemical, there is need to compare the efficiency of biopolymeric nanofluids with their inorganic and metallic polymeric nanofluid counterparts at the same conditions. Therefore, in this study the thermal degradation of crystalline starch nanofluid (CSNF) was compared with SiO_2 polymeric nanofluid (SiO_2PNF) and Al_2O_3 polymeric nanofluid ($\text{Al}_2\text{O}_3\text{PNF}$). The IFT properties of CSNF at oil-water interface and wettability alteration efficiency of CSNF were compared with SiO_2PNF and $\text{Al}_2\text{O}_3\text{PNF}$ at the same conditions. The oil recovery performance of the polymeric nanofluids was compared at typical reservoir conditions (temperature of 120 °C, pressure of 3000 psi and salinity of 22,000 ppm).

2. Materials and methods

2.1. Materials

HPAM with degree of hydrolysis 25 mol%, mol/wt of 20×10^6 Da was acquired from SNF Floerger, Paris. SiO_2 (inorganic nanoparticles) with a

purity of 99.5%, 15–20 nm size and mol/wt 60.8 g/mol was obtained from US Research nanomaterial Inc. USA. Al_2O_3 (metallic nanoparticles) with a purity of 99%, 20 nm size and mol/wt 101.96 g/mol was obtained from Sky Springs Nanomaterials Inc., Houston, TX, USA. CSNP (biopolymeric nanoparticles) with purity >99%, size of 6.97–163 nm was produced from native cassava starch with amylopectin (75 wt%) and amylose (25 wt%) as described by Agi et al. [17,18]. Sodium chloride (NaCl) with 99% purity and mol/wt 58.44 g/mol was obtained from Merck group. An intermediate crude oil from an oilfield in Sarawak, Malaysia (density of 0.8283 g/mL @25 °C, API gravity 37.7 and viscosity of 10 mPa.s @25 °C) was used for the experiments. Three mid-permeability sandstone cores from the same outcrop were utilized for the contact angle and core flooding tests. The physical properties of the sandstone cores are shown in Table 1. The X-ray diffraction (XRD) of the core (Fig. 1) reveals that the samples are mainly quartz (98.9%) and illite (1.1%).

2.2. Methods

2.2.1. Polymeric nanofluids preparation

SiO_2PNF and $\text{Al}_2\text{O}_3\text{PNF}$ were made by a two-stage technique. A 0.1 wt% each of SiO_2 and Al_2O_3 were dispersed in deionized water (DIW) and sonicated for 35 min to form a homogenous dispersion. HPAM (0.1 wt%) was added to the nanofluids dispersion and agitated for 23 h on a stirrer. On the other hand, 0.2 wt% of CSNP was dissolved in DIW, stirred for 6 h and ultrasonicated for 1 h. To investigate the effect of salinity on the polymeric nanofluids, NaCl with different concentrations (0.9–2.2 wt%) was added to the polymeric nanofluid suspension and stirred for 24 h. The salinity range depicts a typical Malay Basin salinity [19].

2.2.2. Characterization of polymeric nanofluids

To determine the microstructures and morphology of the nanoparticles, a transmission electron microscopy (TEM) HITACHI (HT 7700) image analyser was used. Samples were captured at electrical energy of 120 kV. An inbuilt HITACHI EMIP-SP electron microscope image integration software automatically measured the particles sizes and enhanced the images. Shimadzu IR Tracer-100 Fourier transform infrared (FTIR) was utilized to determine the functional groups of CSNP and interaction between SiO_2PNF and $\text{Al}_2\text{O}_3\text{PNF}$ within a scanning range of 500 to 4000 cm^{-1} . A light scattering instrument (Anton Paar Litesizer™ 500) was used to determine stability and surface charge of the polymeric nanofluids. The polymeric nanofluids (0.1 wt%) were dissolved in distilled water (DW) and transferred to omega cuvette for analysis. The analysis was carried out at a back-scattering angle of 170° at 25 °C. The refractive index of water was 1.3303 and the viscosity of water was 0.8903 mPa.s.

2.2.3. Rheological analysis

The rheology of SiO_2PNF , $\text{Al}_2\text{O}_3\text{PNF}$ and CSNF were determined using Brookfield RST rheometer. The rheometer is composed of temperature control connected to water bath for high temperature conditions. All the measurements were carried out at 1–1000 s^{-1} (shear rate) at a temperature range of 26–80 °C. For repeatability, the experiments were conducted in triplicate and the average reported.

Table 1
Properties of sandstone core.

Diameter (cm)	Length (cm)	Bulk Volume (cm^3)	Pore Volume (cm^3)	Porosity (%)	Permeability (mD)
3.7	9.8	100.37	17.00	16.9	201

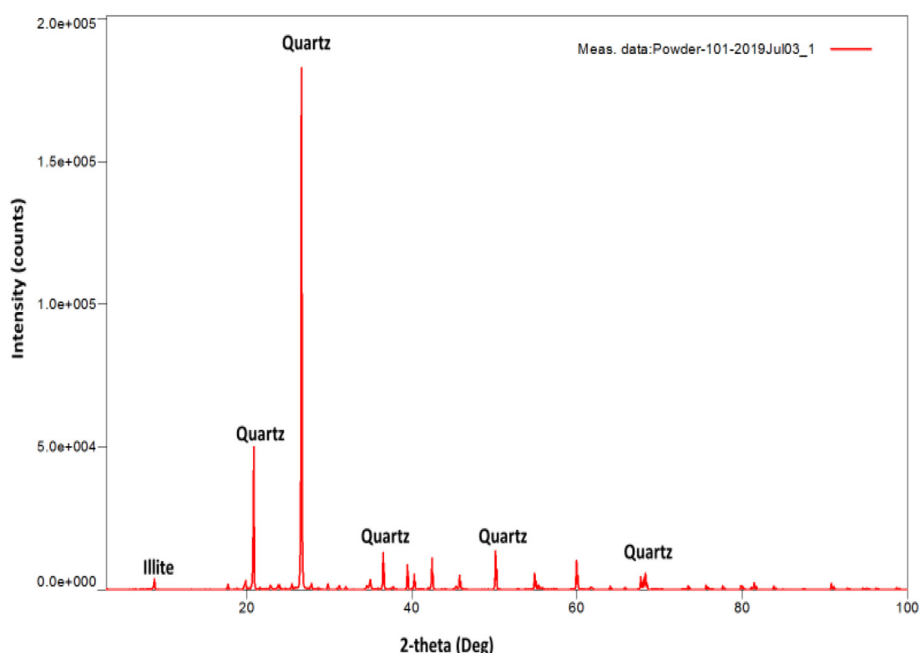


Fig. 1. XRD pattern of sandstone core.

2.2.4. IFT determination

The IFT between SiO_2 PNF, Al_2O_3 PNF, CSNF and oil were determined with Easy Dyne tensiometer (K20) by Kruss GmbH, Germany. It was connected to a water-bath to control temperature of the tensiometer. IFT of polymeric nanofluids at different concentration (0.05–0.2 wt%) as a function of NaCl concentrations (0.9–2.2 wt%) and temperature (26–80 °C) were determined.

2.2.5. Core samples preparation and wettability determination

Core samples of 1 cm thick and 5 cm in diameter with a flat surface were used for the contact angle determination. The cores were washed with DW and toluene to get rid of impurities, and dried for 24 h. The

samples were placed in a beaker and rendered oil-wet by pipetting oil samples on the surface until it was completely immersed in crude oil. The beaker was sealed to prevent evaporation and contamination, and placed in the oven for 78 h at 90 °C. To evaluate the wettability alteration efficiency of SiO_2 PNF, Al_2O_3 PNF and CSNF under static condition, the cores were treated with 0.2 wt% of the polymeric nanofluids for 78 h and dried for 24 h. Wettability alteration before and after treatment with polymeric nanofluids were estimated by determining the contact angles. It was achieved by using a curved needle to place a drop of oil on a horizontally held core as shown in Fig. 2. The images of the drops (26–80 °C) were captured with a digital camera and analysed with image analyser software (Image J 1.48 s) to determine the contact angles.

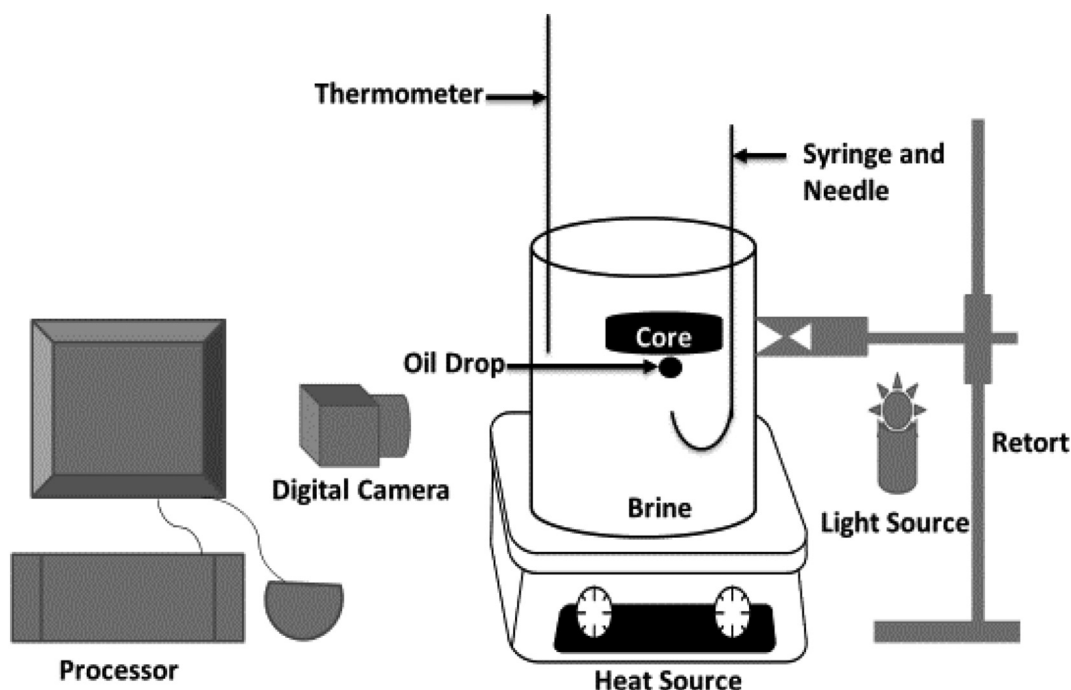


Fig. 2. Experimental setup used for wettability test.

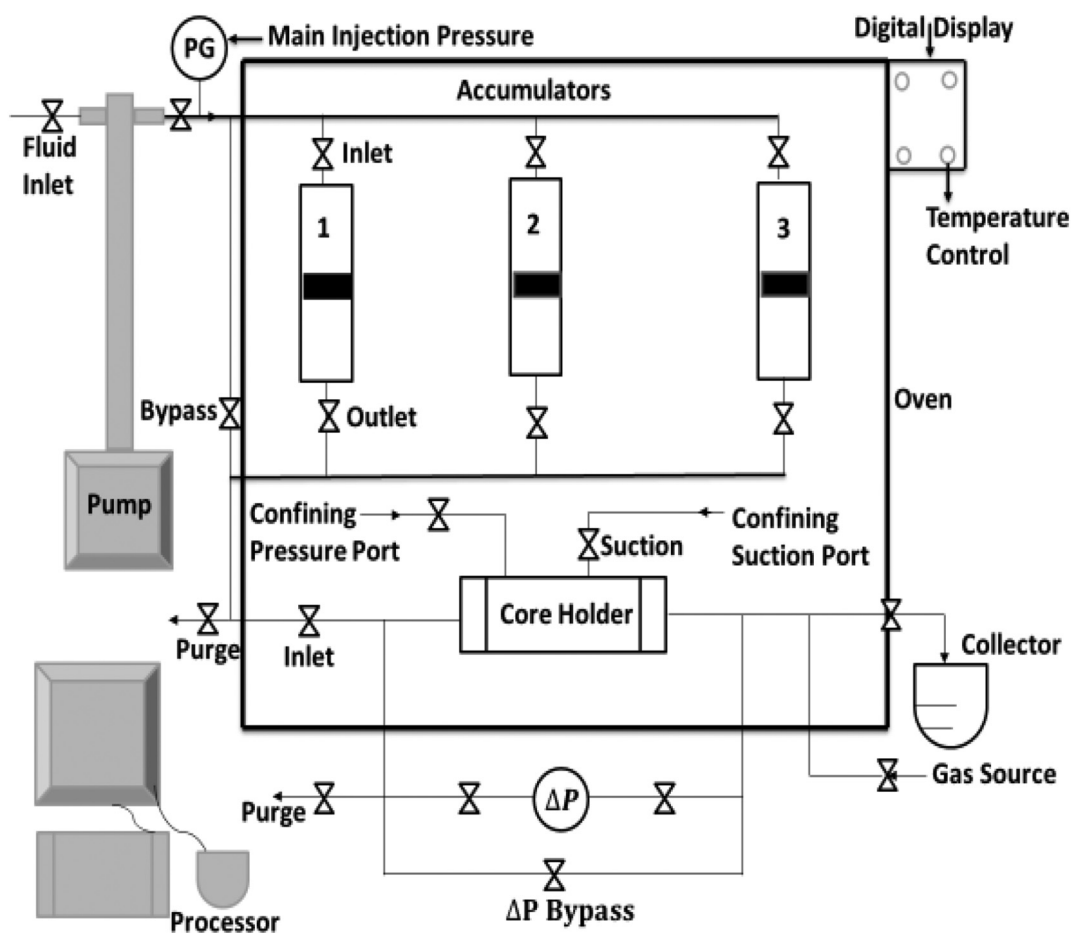


Fig. 3. Schematic representation of core-flood equipment.

2.2.6. Core flooding test

The core flooding was investigated using a high-pressure high-temperature (HPHT) apparatus manufactured by Fars EOR technologies (Fig. 3). The equipment consists of a furnace for temperature regulation,

four accumulators for injecting fluid and a compartment for holding the core. It has a temperature limit of 150 °C and pressure capacity of 6000 psi. Three identical mid-permeability core samples from the same outcrop as that utilized for the contact angle test were utilized

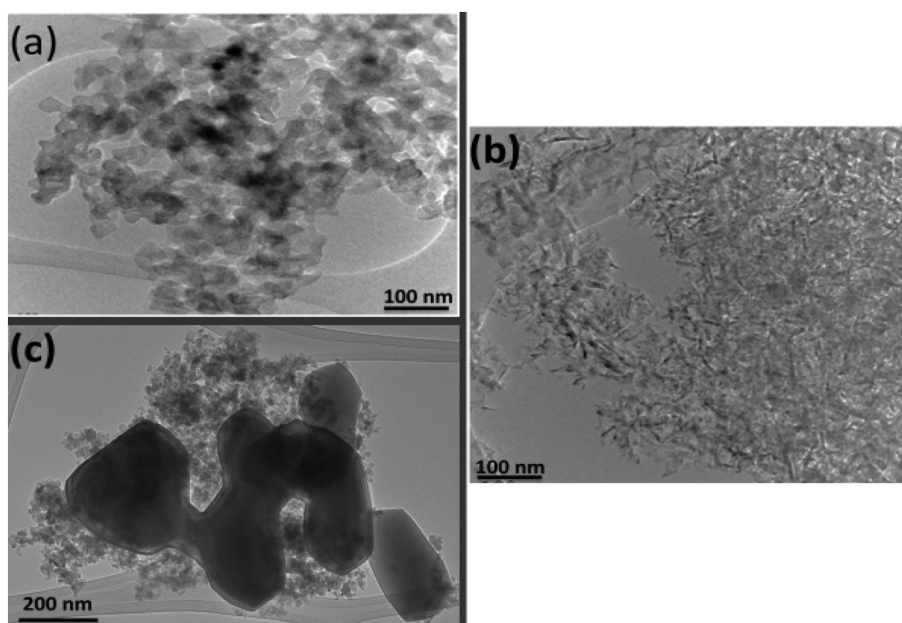
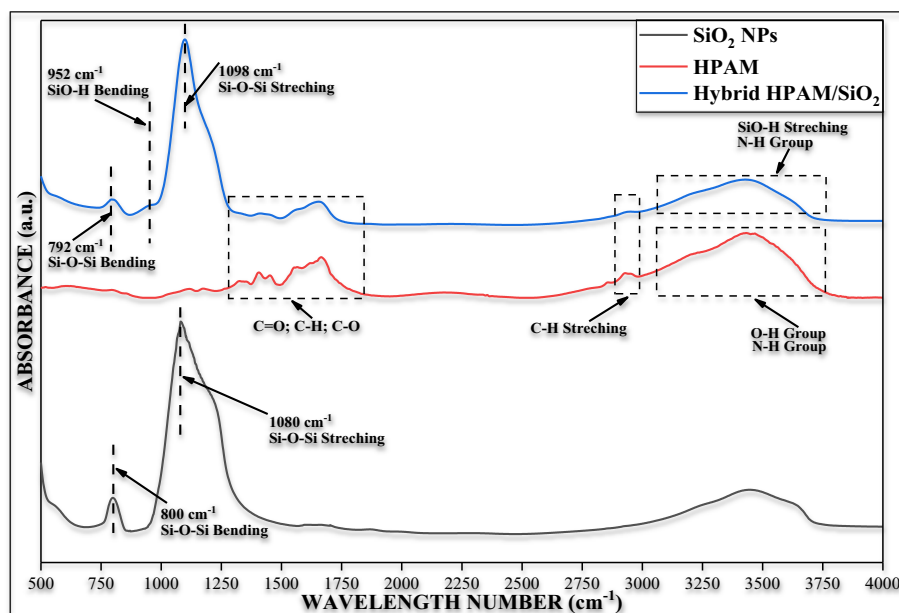


Fig. 4. TEM image of (a) SiO₂ nanoparticles, (b) Al₂O₃ nanoparticles, and (c) CSNP.

Fig. 5. FTIR spectra of SiO₂PNF.

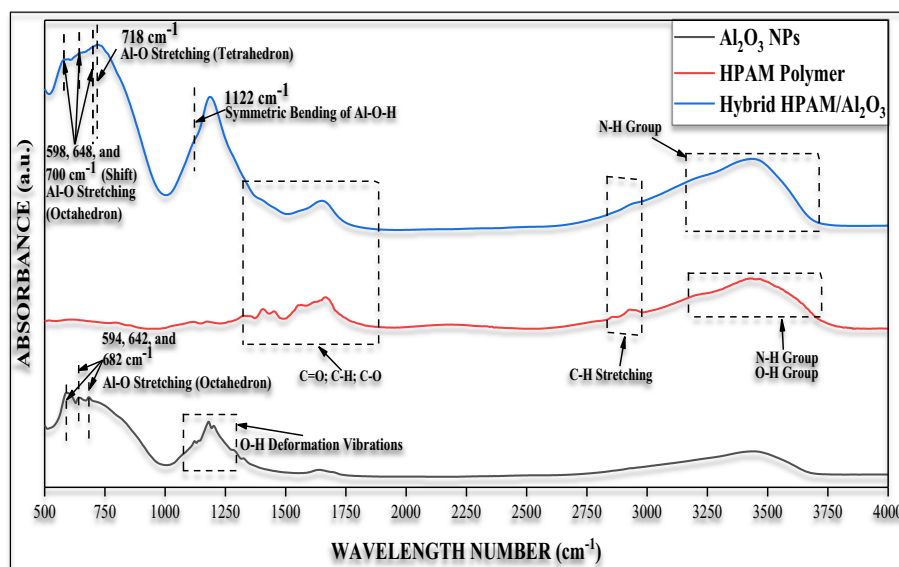
for oil displacement test (Table 1). Core samples were washed with toluene in a Soxhlet distillation extractor column before and after each use, the cores were subsequently dried for 24 h at 95 °C in an oven. Oil displacement tests were executed to determine the oil recovery efficiency of SiO₂ PNF, Al₂O₃ PNF and CPNF. To simulate the reservoir condition of a typical Sarawak oilfield, the equipment was pressured to 3000 psi, supported with a back pressure (100 psi) and oven temperature raised to 120 °C. After vacuuming, the system was saturated with 2.2 wt% of synthetic brine and flooded with oil until connate water was achieved. ISCO pump was utilized in pumping injectants from accumulators to the equipment. Crude oil was introduced into the core at 0.5 mL/min and aged for 24 h to achieve equilibrium. Consequently, water was injected at a constant flow rate until breakthrough occurred. Then, 0.5 PV consisting of 0.2 wt% of different polymeric nanofluids were injected to recover the bypassed oil. Chase water (0.5 PV) was later injected to recover any remaining oil. All the experiments were conducted in duplicate and the average reported.

3. Results and discussion

3.1. Polymeric nanofluids characterization

TEM images of SiO₂, Al₂O₃ and CSNP are shown in Fig. 4. It shows that SiO₂ nanoparticles has a semi-crystalline structure with spherical shape, with sizes ranges from 15 to 20 nm (Fig. 4a). Fig. 4b shows that Al₂O₃ nanoparticles has irregular, spiral shape with size of about 20 nm. On the other hand, CSNP shows spherical crystalline particles of size range 10.1–19.1 nm. The grains formed platy and pear-like shapes (Fig. 4c) of around 163 nm from which smaller particles emerged.

FTIR analysis of the polymeric nanofluids is presented as Figs. 5, 6 and 7. The result of SiO₂PNF in comparison with pure SiO₂ nanoparticles and HPAM are shown in Fig. 5. SiO₂PNF showed two peaks at 1098 cm⁻¹ and 792 cm⁻¹ representing the vibration of Si-O-Si unit. The crest at 962 cm⁻¹ shows the vibration of Si-OH, which was created by the

Fig. 6. FTIR spectra of Al₂O₃PNF.

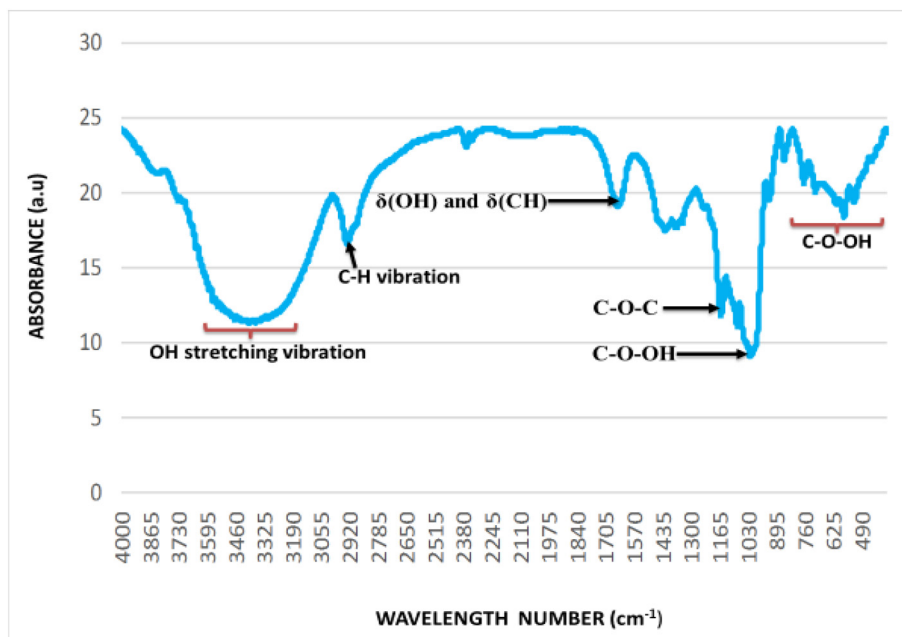


Fig. 7. FTIR spectra of CSNP.

-OH unit on the surface of SiO₂. The OH groups reacted with -COOH, -CHO and -NH₂ on the HPAM to form SiO - H...NH or SiO - H...O - CNH₂ or SiO...HNH - CO - C (strong hydrogen bridges and hydrolysable covalent crosslinks). Whereas the bands at 1350, 1500, and 1650 cm⁻¹ correspond to Si-O, Si-NH₂, and -NH₂, respectively. Broad peak at 3100–3750 cm⁻¹ indicates N-H, -OH, and Si-OH vibration, this interaction between HPAM and SiO₂ nanoparticles resulted to a hybrid SiO₂PNF [11].

Fig. 6 displays the FTIR spectra of Al₂O₃PNF in comparison with Al₂O₃ nanoparticles and HPAM. The peaks at 718 and 1122 cm⁻¹ correspond to tetrahedral shape Al-O and the vibration of Al-O-H which was necessitated by -OH band on the alumina surface. The vibration of the carboxyl unit of HPAM appeared at 1652 cm⁻¹. Also, Al-O - H...N - H or Al-O - H...O - CHNH₂ shows a strong hydrogen link among the -OH unit on Al₂O₃ and oxygen/nitrogen of the amide group present in the HPAM. The hydrogen units in the HPAM and the oxygen unit in the Al₂O₃ formed Al-O...HNH - CO - C hydrogen bonds. This led to a strong hydrolysable crosslink in the Al₂O₃PNF [5].

CSNP showed a broad peak between 3500 and 3200 cm⁻¹ which represent the stretching vibration of OH group of the cellulose present (Fig. 7). The peak at 2930 cm⁻¹ is characteristic of C-H vibration, whereas the crest at 1650 cm⁻¹ represents δ(OH) and δ(CH) adsorption of water. Peak at 1650 cm⁻¹ corresponds to the C=O band of the carboxyl and carbonyl groups. The stretching vibration C-O-C was observed at 1158 cm⁻¹. The D-glycopyran group, C-O and attached OH was observed between 1080 and 709 cm⁻¹.

Colloidal stability of polymeric nanofluids dispersion can be envisaged by the magnitude of the zeta potential. To determine the stability of the polymeric nanofluids, the zeta potential with time was determined. The results (Fig. 8) show negligible variation in the values of the zeta potential with time and the error bar shows that the uncertainty is minimal which confirms the repeatability of the experiments. Moreover, the polymeric nanofluid was still stable as no rapid coagulation or flocculation was observed. This could be because of the repulsive interaction or electrostatic forces between the suspended particles that impeded the aggregation and agglomeration of the particles thereby rendering it stable [20]. The slight shift in the zeta potential result is due to the difference in the location of the slipping plane of the polymeric nanofluids and the presence of disassociated carboxylic groups [21–23]. The negative value of the Al₂O₃PNF confirms the success of

the surface coating with HPAM. CSNF showed higher surface charge compared to SiO₂PNF and Al₂O₃PNF. This could be attributed to microfluidization of the CSNP, which led to the higher zeta potential [18]. It might also be due to the replacement of the hydroxyl group by the sulfate ester group (-OSO₃⁻) during synthesis of CSNP that produced an electrostatic repulsion. Therefore, it can be concluded that the presence of these randomly distributed negative charge surface ester groups on the surface of CSNP and the disassociation of the remaining valences contributed to the high zeta potential which contributed to its stability.

3.2. Comparison of the rheology of polymeric nanofluids

The flow performance of SiO₂PNF, Al₂O₃PNF and CSNF at the same concentration (0.2 wt%) were compared. All the polymeric nanofluids exhibited pseudoplastic and shear thinning at high and low shear rates (Fig. 9). This might be due to strong electrostatic hydrogen linkage between silanol group and the HPAM, and the covalent linkages of the aluminol functional group and HPAM amino group [5,6]. However, the viscosity of CSNF was greater than SiO₂PNF and Al₂O₃ at the same concentration. It might be because of the electroviscous negative charge on the surface of the CSNP and the formation of a stronger particle-particle

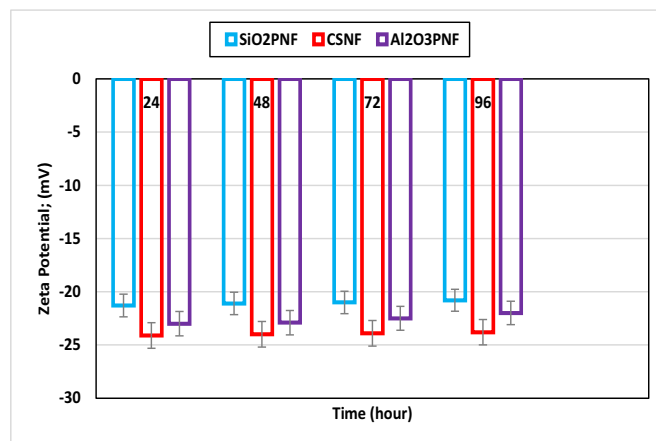


Fig. 8. Zeta potential of polymeric nanofluids.

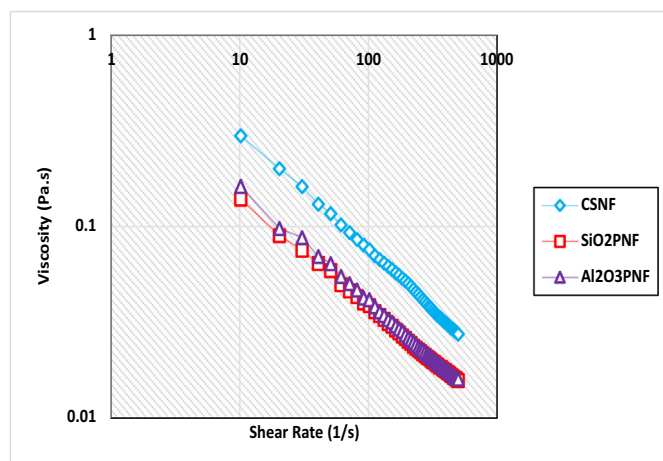


Fig. 9. Apparent viscosity of polymeric nanofluids.

hydrogen bonds compared to that formed by silanol and aluminol group on HPAM. The result is coherent with previous work of Shafiei-Sabet et al. [24]. They reported that the rheological properties of cellulose nanocrystals vary due to their surface charge and ionic strength.

3.3. Impact of salinity on viscosity of polymeric nanofluids

Reservoir brine poses a serious problem on flow behaviour of injected EOR fluids. Therefore, a comparative study on the salinity resistance of SiO₂PNF, Al₂O₃PNF and CSNF were investigated. The results (Fig. 10) show that the viscosity of the polymeric nanofluids reduced as concentration of NaCl increased. Which might be because of screening effect of Na⁺ which reduced the repulsive energy of the polymeric nanofluids and the hydrodynamic volumes of the polymeric nanofluid subsequently reducing viscosity [18,25]. All the polymeric nanofluids still retained their pseudoplastic and shear-thinning behaviour as salinity increases. This behaviour can be likened to the uniformity of the polymeric nanofluids as shear rate increases, as initially agglomerated nanoparticles begins to separate [26]. But the effect of salinity was mild for CSNF compared to SiO₂ and Al₂O₃. This is because of the electric double layer (EDL) and reduction in Debye's length of CSNF compared to SiO₂PNF and Al₂O₃PNF. EDL force are repulsive in nature therefore, they decreased the agglomeration of the CSNP and hence the stability of the CSNF [20]. This was necessitated by the higher collision among the CSNP which affected the presence of the salt [27].

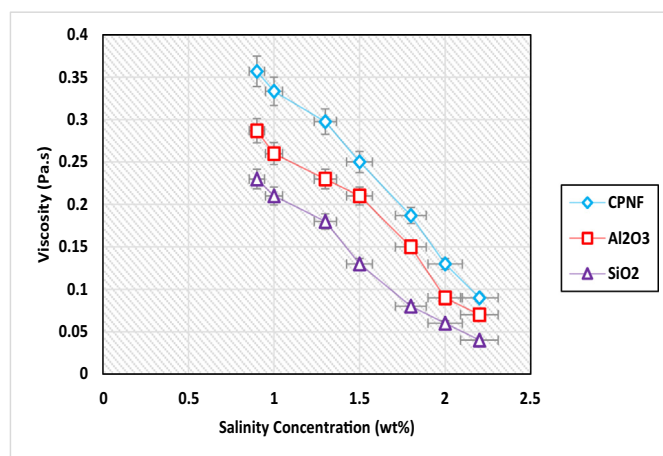


Fig. 10. Effect of salinity on the apparent viscosity of polymeric nanofluids.

3.4. Thermal degradation of polymeric nanofluids

The thermal degradation of a material is very important when determining the energy needed to overpower the activation energy of flow as material moves from one equilibrium to another. Fig. 11 shows the effect of temperature (26–80 °C) on the viscosity of the polymeric nanofluids at the same concentration (0.2 wt%). The results show that the viscosities of the polymeric nanofluids are dependent on temperature. The viscosities of SiO₂PNF and Al₂O₃PNF declined as temperature increased [28]. This is because decrease in adsorption of HPAM on SiO₂ and Al₂O₃ nanoparticles. As temperature increases, there is dihydroxylation of hydrogen bond on the silanol and aluminol group that weakened the structure of the SiO₂PNF and Al₂O₃PNF which might have induced a hydrophobic nature and resulted in the decrease in viscosity [4]. The viscosity of Al₂O₃PNF was higher compared to SiO₂PNF. This is because of the formation of COO⁻ group during hydrolysis of HPAM at high temperature, which necessitated the continuous adsorption of HPAM on Al₂O₃ due to the electrostatic interaction of Al³⁺ and COO⁻. Whereas there was no interaction between the negatively charged SiO₂. The CSNF showed a reversed trend in comparison with SiO₂PNF and Al₂O₃PNF, as the temperature increases the viscosity increased. This could be because of increase in tensile strength due to binding of the CSNF which might have initiated a strong cohesive bond between the CSNP [29]. It might also be due to the formation of a three-dimensional (micelle type) network of flocs after the synthesis of CSNP that resulted in the increase of viscosity. Furthermore, heating induces the melting CSNP crystal into their composing molecules which might have resulted to increase in viscosity [30,31]. Also, heating might have caused expansion and disruption of inter and intra molecular hydrogen bond in the CSNP and increased the starch-water hydrogen bond. Consequently, the increase in temperature of the CSNF facilitated swelling of the CSNP [27]. Owing to the fact that during the acidolysis process only the non-crystalline area of the starch was destroyed, the crystalline area was preserved, which basically keeps the same crystal structure as that of the native starch. This is consistent with earlier work of Xiao et al. [32] where they reported that the inter and intra molecular hydrogen bond of native starch breaks with increase in temperature and the crystal structure disappears resulting in a sharp rise in viscosity. The result shows that even at high temperature the interaction between the CSNP still exist which demonstrated the thermal stability of CSNP when it is propagated through oil field reservoirs. The uncertainty of the experimental results (Figs. 10 and 11) is shown by the error bar which indicates that the uncertainty is rather small, and the difference is not significant.

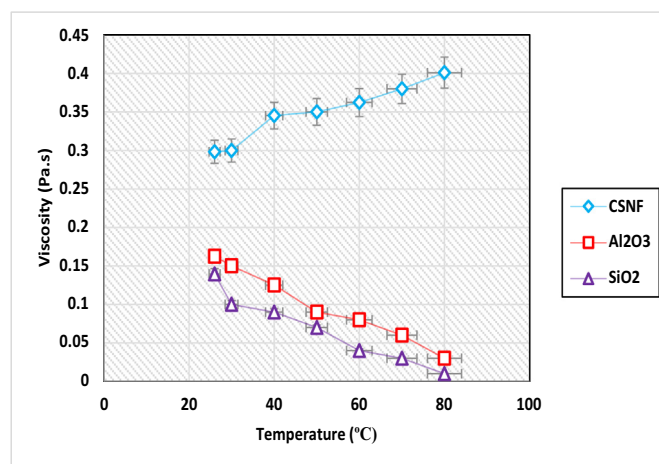


Fig. 11. Effect of temperature on polymeric nanofluids.

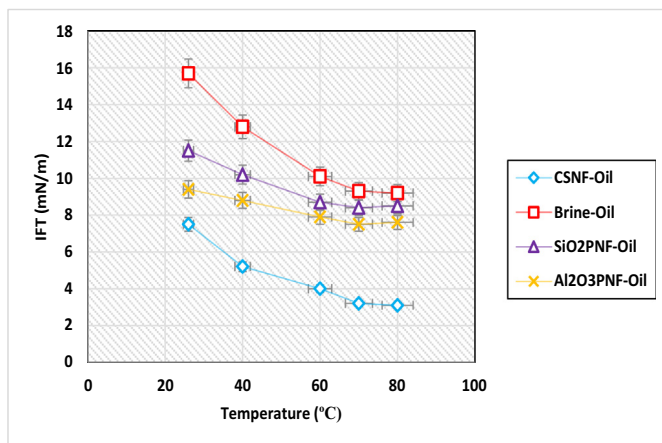


Fig. 12. IFT of polymeric nanofluid in the presence of brine (2.2 wt%) as a function of temperature.

3.5. Impact of polymeric nanofluids on IFT

IFT between trapped oil and displacing fluid plays a significant role in oil recovery. Reducing IFT decreases severity at the interface and allows deformation of the O/W interface, which leads to improved oil recovery. Nanofluids have been reported to reduce IFT. The interfacial properties strongly hinges on the quality of surface-active agent which moves to the interface of O/W. Besides, the movement of this surface-active agent from bulk to the interface depends on the medium temperature. Therefore, the influence of temperature (26–80 °C) on adsorption of surface-active agents formed from SiO₂PNF, Al₂O₃PNF and CSNF at the interface of oil and brine (2.2 wt%) were studied. Fig. 12 shows the IFT of SiO₂PNF, Al₂O₃PNF and CSNF compared to brine as a function of temperature, with standard error bar almost the same. This signifies certainty that the mean computed value estimated the true mean value of the experimental results. The results show that there is a

significant decrease in IFT in the presence of polymeric nanofluids compared to brine alone. It could be credited to the electrostatic interaction of the polymeric nanofluids and brine in the bulk, which increases the dispersion of the polymeric nanofluids to the interface of O/W [33]. The interaction between the polymeric nanofluids in the presence of brine was found to be lower than that of brine alone (Fig. 12). This singularly confirms the formation surface-active agent from electrostatic attraction between polymeric nanofluids and brine which could have significantly reduce O/W IFT compared to brine alone. Therefore, it can be concluded that impact of electrostatic attraction is foremost over the effect of electrostatic repulsion in decreasing IFT.

As the temperature of the polymeric nanofluid increases, the liquid molecules had higher kinetic energy, there was a rapid migration of polymeric nanofluid from the bulk to the O/W interface. This can be attributed to thermophoresis phenomenon of the nanofluids which migrated the particles from a region of high temperature (hot zone) to a region with lower temperature (cold zone) [20,34]. This led to a significant adsorption of the polymeric nanofluid at the interface resulting in a charged EDL which decreased the coating at the interface. The arrangement of the polymeric nanofluids at the interface will increase the number of impurities, but in brine the impurities are salted off [35]. This weakens the cohesive energy and expands the intermolecular energies at the interface thereby reducing IFT of the polymeric nanofluids.

However, IFT of SiO₂PNF and Al₂O₃PNF at the interface of O/W showed a non-monotonic tendency as temperature increased. It was observed that IFT of SiO₂PNF and Al₂O₃PNF decreased to 8.4 ± 0.25 mN/m and 7.5 ± 0.22 mN/m respectively as the temperature was increased to 70 °C. A further increase in temperature (80 °C) of the system increased the IFT. This is because as the temperature increases, it promotes the detachment of the HPAM from the nanoparticles and promotes only the migration/adsorption of the nanoparticles at the interface (Fig. 13). As temperature increases SiO₂PNF and Al₂O₃PNF begin to desorb from the interface because of thermal instabilities. This indicates that at higher temperature, there were increased chances of aggregation and consequently a decreased activity at the interface

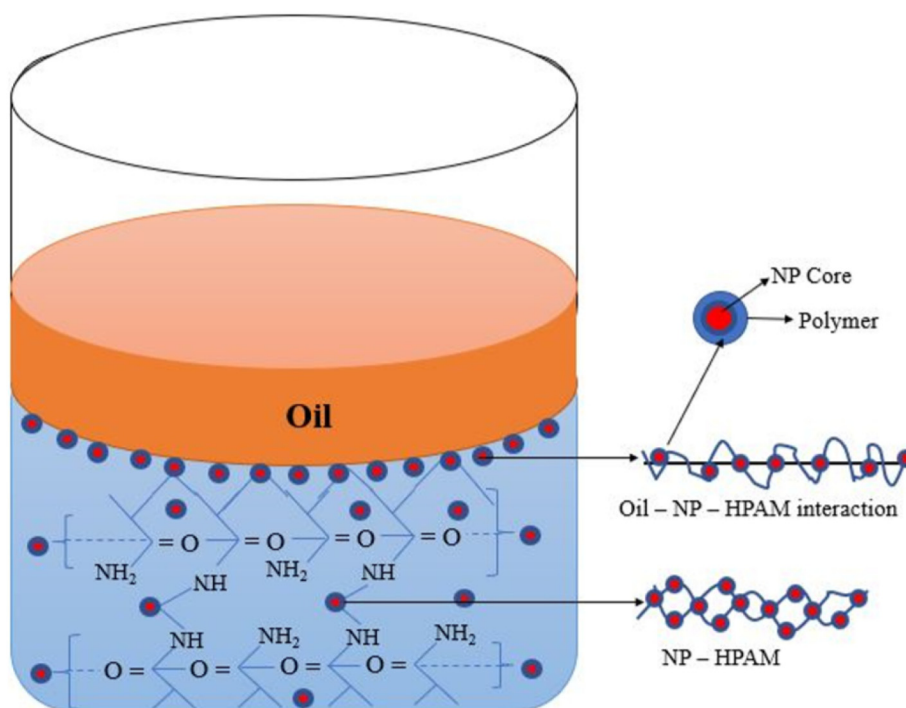


Fig. 13. Mechanism of IFT reduction in the presence of SiO₂PNF and Al₂O₃PNF.

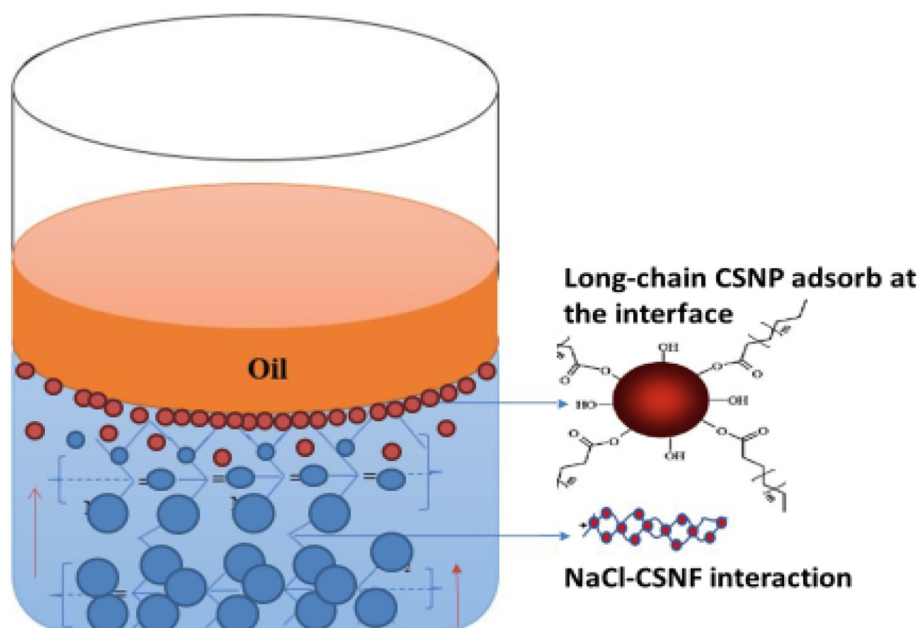


Fig. 14. Mechanism of IFT reduction in the presence of CSNF.

[36]. This is coherent with prior work of Gbadamosi et al. [6]. They also observed a sudden increase in IFT, which implies that the surface-active agent at the interface has diminished due to desorption.

The IFT of CSNF continued to decrease even at higher temperature of 80 °C and it showed the lowest IFT at all temperatures (Fig. 12). This might be due to the breakage of larger droplet to smaller ones as temperature increases (cavitation) and the increase in hydrophobicity of the CSNF [25,37]. Temperature increased the free energy per unit surface area at the interface for CSNF compared to SiO₂PNF and Al₂O₃PNF [33]. The result is consistent with rheology result (Fig. 11) as increase in temperature created a three-dimensional network that increased the viscosity. The long chain CSNP arranged themselves at the interface (Fig. 14) hindering the development of anisotropic phase in the CSNF and induced the creation of EDL which reduced the layer of interface and IFT.

3.6. Impact of polymeric nanofluids on wettability alteration

Wettability controls displacement of wetting and non-wetting phase of fluid at pore-scale. As such a change in the wettability from oil-wet to water-wet can enhance fluid flow. However, reservoir salinity can affect the stability of injected fluid and temperature can affect the wetting of solid surface. It is, therefore, important to investigate the impact of salinity and temperature on different polymeric nano-modified sandstone surfaces. To achieve this, the influence of SiO₂PNF, Al₂O₃PNF and CSNF (0.2 wt%) on the wettability alteration of oil-wet sandstone at reservoir salinity (2.2 wt%) and different temperatures (26–80 °C) were investigated. The results show the reference angles of the sandstone core to be 114 and 144 degrees (Fig. 15).

The wettability of oil wet cores was altered to water-wet when treated with polymeric nanofluids (Fig. 15). This might be because of polymeric nanofluid adsorption on sandstone surface that altered wettability. This is because of the disassociation of the two atoms of Na and Cl to form Na⁺ and Cl[−] ions. The quartz in the sandstone core (Fig. 1) attracts Na⁺ to form a layer on sandstone core, the high concentration of NaCl (2.2 wt%) means excess of positive Na⁺ ions on the sandstone surface to attract the negative parts of polar components present in crude oil. However, the monovalent ions of Na⁺ covering the sandstone core prevented contact between crude oil and sandstone core. As a result of this interaction, the film present on the sandstone core

surface was not disrupted by bases or acids in the crude oil. Therefore, this might be the main reason which might have altered the wettability.

The reduction of contact angle as temperature increases confirms stability of nanofluids when it is propagation in porous medium. Temperature reduces the number of active sites on the sandstone core which might have influenced the spreading behaviour of the polymeric nanofluids [25]. The dispersion of the polymeric nanofluids front increases as temperature increased, temperature break-down the bonds and water molecules desolvated the polymeric nanofluids, this might have increased the attraction of the sandstone surface to the polymeric nanofluids [38]. Furthermore, the heat and mass transfer of the nanoparticles might have been enhanced due to the micro-conventional and mechanical agitation induced by Brownian motion of the polymeric nanofluids [20,34]. Also, temperature decreases asphaltene precipitation which is washed out from the sandstone surface by the adsorbing polymeric nanofluids. The nanoparticles could make asphaltene suspended in the oil and rapidly adsorb them thereby inhibiting them from being precipitated [39]. This is coherent with earlier findings of Akbarzadeh et al. [40] and Escrochi et al. [41]. They stated that above the bubble point pressure, more asphaltene is in liquid phase therefore

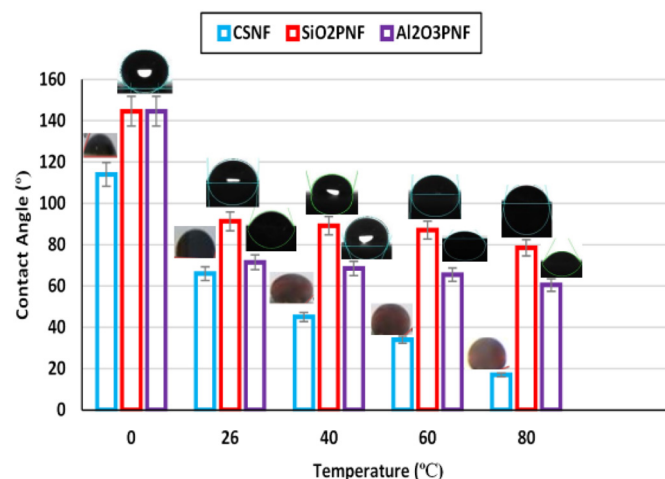


Fig. 15. Oil contact angles and microscopic image of oil drops at different temperatures.

for a saturated and single-phase reservoir, increases in temperature will increase asphaltene solubility so its precipitation decreases, and the reservoir become water wet. CSNF showed better potential to alter wettability compared to SiO_2PNF and $\text{Al}_2\text{O}_3\text{PNF}$ at all conditions. This could be attributed to a better electrostatic attraction and high affinity of CSNF to adsorb on sandstone surface. It might also be due to steric force which led to adsorption of the organic molecules on the sandstone surface [20]. It can therefore be concluded from this study that SiO_2PNF and $\text{Al}_2\text{O}_3\text{PNF}$ had a lower adsorption on sandstone surface which resulted to a low reduction in contact angle. The standard error of the contact angle and temperature were determined for three tests. The error bars were used to determine the positive and negative standard error from the mean of the contact angle and temperature. It was observed from the error bar (Fig. 15) that the results show good parallelism, indicating that the experimental results are reliable.

3.7. Oil displacement results

To determine the efficiency, effective treatment methods and the potentials of the polymeric nanofluids for EOR, series of core flooding experiments were performed to mimic water flooding and polymeric nanofluid flooding of a Sarawak oil field. The difference in cumulative oil recovery in the secondary and tertiary recovery modes are presented in Fig. 16. Water flooding recovered 48% OOIP, which signifies that sufficient quantity of oil was bypassed. Tertiary recovery was initiated, and oil recovery increased by 13%, 17% and 23% with SiO_2PNF , $\text{Al}_2\text{O}_3\text{PNF}$ and CSNF, respectively. This is because the polymeric nanofluid blocked the permeable channels created by water flooding and recovered additional oil from small pores [42]. The reduction in IFT between the O/W facilitated the mobilization of the initially bypassed oil. The results are consistent with IFT and wettability result, which decreased as temperature increased. It therefore shows that the polymeric nanofluid were still stable at high salinity (2.2 wt%) and HPHT (3000 psi, 120 °C) reservoir conditions.

The pressure drop profile shows a good relationship with recovery result (Fig. 17). When waterflood commenced, there was a rise in pressure drops, followed by a decline until it became constant. The reason for the declining trend is due to the high mobility of water compared to oil, which was evident as breakthrough time saw the pressure drop remain constant. A favourable type of displacement will occur if

$$\frac{k_{rw}\mu_w}{k_{ro}\mu_o} = M \leq 1 \quad (1)$$

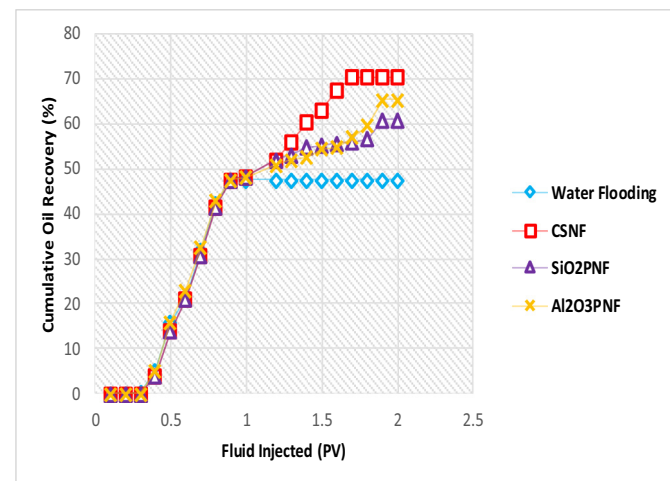


Fig. 16. Cumulative oil recovery of polymeric nanofluids.

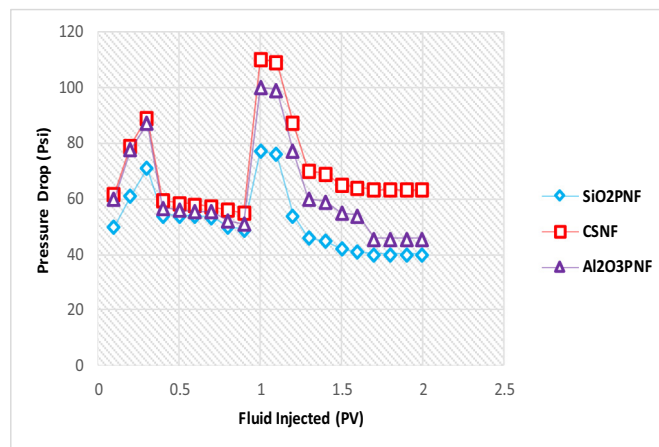


Fig. 17. Pressure drop of polymeric nanofluids.

whereas, M is mobility ratio, μ_o is viscosity of oil (mPa.s), μ_w is viscosity of water (mPa.s), k_{ro} and k_{rw} are end point relative permeabilities of oil and water respectively (mD). Mobility ratio was determined using the method of Bamidele et al. [43] and it was observed that the mobility ratio of water flooding approaches unity faster than that of SiO_2PNF , $\text{Al}_2\text{O}_3\text{PNF}$ and CSNF (Fig. 18). This might have resulted in by-passing of oil and consequently early breakthrough in the water flooding, which is consistent with pressure drop profile (Fig. 17). The delay in approaching unity for SiO_2PNF , $\text{Al}_2\text{O}_3\text{PNF}$ and CSNF signifies that the oil viscosity variation is less than their viscosity variation resulting in a favourable mobility. EOR also saw an increase in the profile, the rise during tertiary recovery is due to their improved viscosity compared to water [42].

Increase in pressure drop as polymeric nanofluid were introduced also demonstrated that the polymeric nanofluids lowered the capillary forces holding the oil in pore spaces [44,45]. The pressure drops remained very high even at elevated temperature which confirms that the polymeric nanofluids were still stable and oil displacement efficiency was still very active at 120 °C, which resulted to increased oil recovery. As the nanofluids imbibe into the sandstone core to expel trapped oil, the pressure profile began to build leading to the formation of O/W emulsion (Fig. 19). This agrees with earlier work of Pei et al. [46] who stated that O/W emulsion enhanced the sweep efficiency by blocking the channel created by water and lowered the oil mobility.

The emulsion generated was examined with an Amscope microscope (Fig. 20). Emulsions generated by SiO_2PNF and $\text{Al}_2\text{O}_3\text{PNF}$ (Fig. 20a and b respectively) showed large drops sizes with high-level

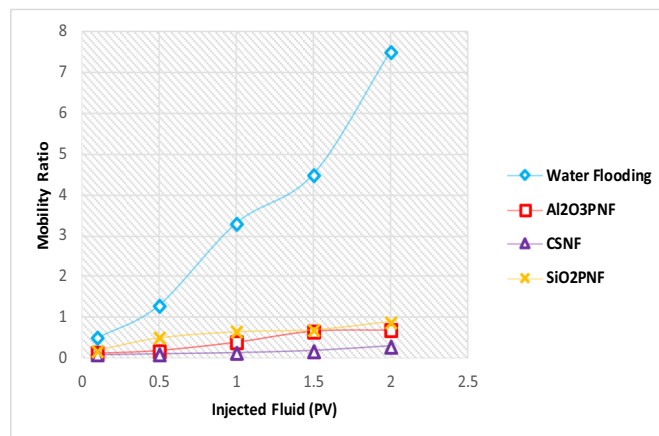


Fig. 18. Mobility ratio of polymeric nanofluids.

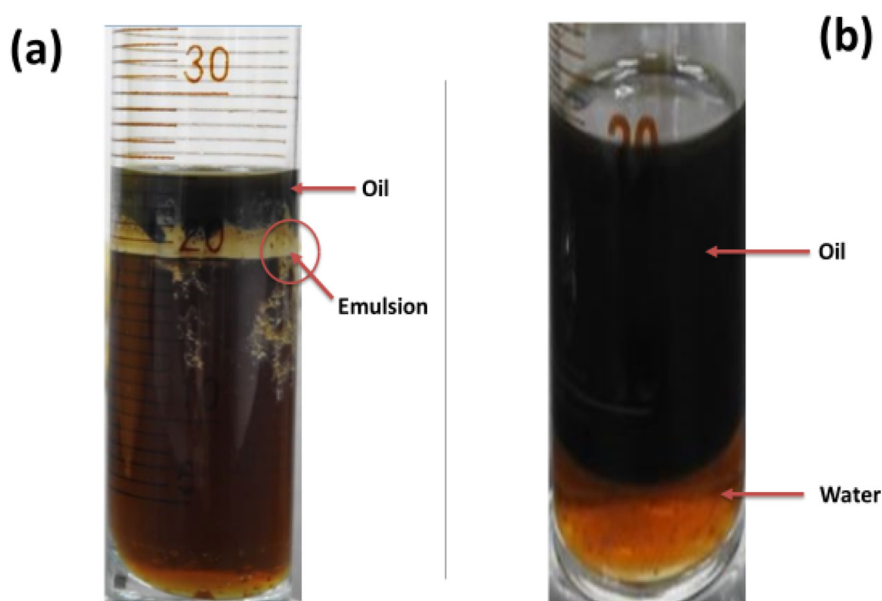


Fig. 19. Emulsion generated during (a) polymeric nanofluid flooding (b) water flooding.

of coalescence compared to CSNF emulsion (Fig. 20c) which has small diameter droplets which signifies stability of the emulsion over a long period, which is consistent with the zeta potential result with time (Fig. 8). This agrees with the recovery results as this singular phenomenon might be one of the reasons for the higher recovery of CSNF compared to SiO_2PNF and $\text{Al}_2\text{O}_3\text{PNF}$. The result also confirmed the ability of CSNF to withstand high temperature degradation compared to SiO_2PNF and $\text{Al}_2\text{O}_3\text{PNF}$, which is consistent with the thermal degradation results (Fig. 11). This agrees with prior work by Hatscher [47] who stated that at a temperature of 135 °C, the viscosity of biopolymer schizophyllan was still stable and the stability lasted for 300 days under anaerobic conditions. The biopolymer also exhibited superb laboratory and field pilot test results in comparison with xanthan and sulfonated polyacrylamide.

4. Conclusions

The present study is focused on comparing the EOR mechanisms and oil displacement behaviour of inorganic, metallic, and bio-polymeric nanofluids which are promising for EOR applications. The morphology of the nanoparticles was determined using TEM, whereas FTIR was used to determine the functional group and interaction between the polymeric nanofluids. Also, the stability of the polymeric nanofluids with time was determined by zeta potential. The thermal degradation

and EOR mechanisms of the polymeric nanofluids were compared and related to the oil displacement ability of the polymeric nanofluids. Based on the experimental results the following conclusions were reached.

1. The surface chemistry of polymeric nanofluids shows possible interaction with other EOR materials and zeta potential results show stability of the polymeric nanofluids.
2. The results show that the viscosities of the polymeric nanofluids are dependent on temperature. The viscosities of SiO_2PNF and $\text{Al}_2\text{O}_3\text{PNF}$ decreased with increase in temperature whereas the viscosity of CSNF increased with increase in temperature.
3. The polymeric nanofluids show good potential in decreasing IFT. Meanwhile, the IFT of SiO_2PNF and $\text{Al}_2\text{O}_3\text{PNF}$ showed a non-monotonic trend with increases in temperature.
4. CSNF showed better potential to alter wettability compared to SiO_2PNF and $\text{Al}_2\text{O}_3\text{PNF}$ at all conditions.
5. A range of 13–23% incremental oil recovery was achieved with the use of polymeric nanofluid. The microscopic image of the emulsion generated shows stability of the emulsion over a long period and confirmed the ability of CSNF to withstand high temperature degradation compared to SiO_2PNF and $\text{Al}_2\text{O}_3\text{PNF}$. The study suggests that the CSNF could be used as an appropriate substitute to conventional CEOR materials.

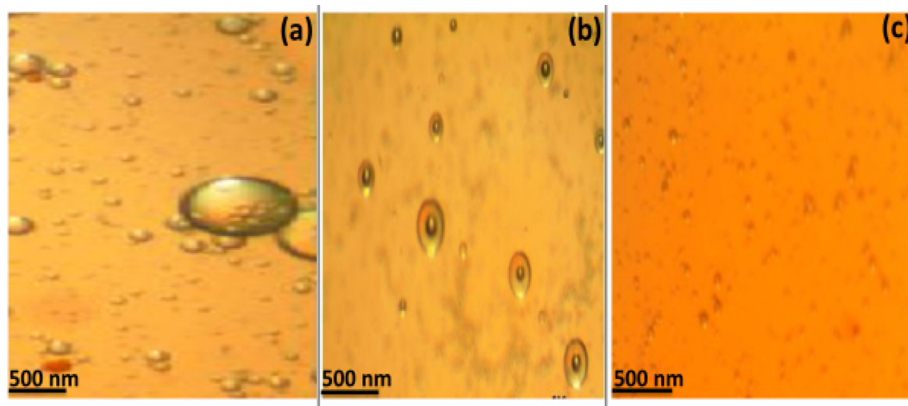


Fig. 20. Microscopic image of emulsion generated during (a) SiO_2PNF flooding, (b) $\text{Al}_2\text{O}_3\text{PNF}$ flooding, and (c) CSNF flooding.

CRediT authorship contribution statement

Augustine Agi: Conceptualization, Methodology, Formal analysis, Investigation, Data curation, Writing - original draft, Visualization. **Radzuan Junin:** Conceptualization, Methodology, Validation, Resources, Visualization, Supervision, Funding acquisition. **Afeez Gbadamosi:** Conceptualization, Formal analysis, Investigation, Data curation. **Muhammad Manan:** Methodology, Validation, Resources, Visualization, Supervision. **Mohd Zaidi Jaafar:** Methodology, Validation, Resources, Visualization, Supervision, Funding acquisition. **Mohammed Omar Abdullah:** Methodology, Validation, Resources, Visualization, Supervision. **Agus Arsad:** Methodology, Validation, Resources, Supervision, Funding acquisition. **Nur Bashirah Azli:** Software, Investigation, Resources, Project administration. **Muslim Abdurrahman:** Methodology, Formal analysis, Resources. **Faruk Yakasai:** Software, Data curation.

Declaration of competing interest

The authors have no conflict of interest.

Acknowledgements

The authors would like to thank the Ministry of Higher Education, Malaysia and Universiti Teknologi Malaysia for supporting this research through Research Management Grants Vot. No. R/J130000.3551.07G52&06G69, R/J130000.2451.08G93, R/J130000.3051.01M99, and R/J130000.7351.4B545.

References

- [1] A.O. Gbadamosi, J. Kiwalabye, R. Junin, A. Augustine, A review of gas enhanced oil recovery schemes used in the North Sea, *Journal of Petroleum Exploration and Production Technology* 8 (4) (2018) 1373–1387.
- [2] A.O. Gbadamosi, R. Junin, M.A. Manan, A. Agi, A.S. Yusuff, An overview of chemical enhanced oil recovery: recent advances and prospects, *International Nano Letters* (2019) 1–32.
- [3] A. Abbas, A. Moslemizadeh, W.R. Sulaiman, M.Z. Jaafar, A. Agi, An insight into di-chain surfactant adsorption onto sandstone minerals under different salinity-temperature conditions: chemical EOR applications, *Chem. Eng. Res. Des.* 153 (2020) 657–665.
- [4] G.A. Pope, Recent developments and remaining challenges of enhanced oil recovery, *J. Pet. Technol.* 63 (07) (2011) 65–68.
- [5] A. Gbadamosi, R. Junin, M. Manan, A. Agi, J. Oseh, J. Usman, Synergistic application of aluminium oxide nanoparticles and oilfield polyacrylamide for enhanced oil recovery, *J. Pet. Sci. Eng.* 182 (2019), 106345.
- [6] A. Gbadamosi, R. Junin, M. Manan, A. Agi, J. Oseh, J. Usman, Effect of aluminium oxide nanoparticles on oilfield polyacrylamide: rheology, interfacial tension, wettability and oil displacement studies, *J. Mol. Liq.* 296 (2019), 111863.
- [7] A. Agi, R. Junin, A. Gbadamosi, Tailoring of nanoparticles for chemical enhanced oil recovery, *International Journal of Nanomanufacturing* 16 (2) (2020) 107–147.
- [8] A.O. Gbadamosi, R. Junin, M.A. Manan, A. Agi, J. Oseh, Nanotechnology Application in Chemical Enhanced Oil Recovery: Current Opinion and Recent Advances, *IntechOpen*, 2019 1–20.
- [9] A. Maghzi, A. Mohebbi, R. Kharat, M.H. Ghazanfari, An experimental investigation of silica nanoparticles effect on the rheological behavior of polyacrylamide solution to enhance heavy oil recovery, *Pet. Sci. Technol.* 31 (2013) 500–508.
- [10] N. Lai, X. Guo, N. Zhou, Q. Xu, Shear resistance properties of modified nanoSiO₂/AA/AM copolymer oil displacement agent, *Energies* 9 (2016) 1037.
- [11] Z. Hu, M. Haruna, H. Gao, E. Nourafkan, D. Wen, Rheological properties of partially hydrolyzed polyacrylamide seeded by nanoparticles, *Ind. Eng. Chem. Res.* 56 (2017) 3456–3463.
- [12] A.O. Gbadamosi, R. Junin, M.A. Manan, N. Yekeen, A. Augustine, Hybrid suspension of polymer and nanoparticles for enhanced oil recovery, *Polym. Bull.* 76 (12) (2019) 6193–6230.
- [13] M.A. Haruna, S. Pervaiz, Z. Hu, E. Nourafkan, D. Wen, Improved rheology and high-temperature stability of hydrolyzed polyacrylamide using graphene oxide nano-sheet, *J. Appl. Polym. Sci.* 47582 (2019) 1–13.
- [14] A. Agi, R. Junin, A. Gbadamosi, Mechanism governing nanoparticles flow behaviour in porous media: insight for enhanced oil recovery applications, *Int Nano Lett* 8 (2) (2018) 49–77.
- [15] B. Wei, Q. Li, J. Ning, Y. Wang, L. Sun, W. Pu, Macro and micro scale observation of a surface functionalized nanocellulose based on aqueous nanofluid in chemical enhanced oil recovery (C-EOR), *Fuel* 236 (2019) 1321–1333.
- [16] S.N. Molnes, I.P. Torrijos, S. Strand, K.G. Paso, K. Syverud, Sandstone injectivity and salt stability of cellulose nanocrystals (CNC) dispersions—premises for use of CNC in enhanced oil recovery, *Ind. Crop. Prod.* 93 (2016) 152–160.
- [17] A. Agi, R. Junin, A. Gbadamosi, A. Abbas, N.B. Azli, J. Oseh, Influence of nanoprecipitation on crystalline starch nanoparticle formed by ultrasonic assisted weak-acid hydrolysis of cassava starch and the rheology of their solutions, *Chemical Engineering and Processing-Process Intensification* 142 (2019), 107556.
- [18] A. Agi, R. Junin, A. Arsad, A. Abbas, A. Gbadamosi, N.B. Azli, J. Oseh, Ultrasonic-assisted weak-acid hydrolysis of crystalline starch nanoparticles for chemical enhanced oil recovery, *Int. J. Biol. Macromol.* 148 (2020) 1251–1271.
- [19] A. Agi, R. Junin, A.Y.M. Alqatta, A. Gbadamosi, A. Yahya, A. Abbas, Ultrasonic ultrafiltration process for the emulsification of oil field produced water treatment, *Ultrason. Sonochem.* 51 (2019) 214–222.
- [20] O. Mahian, L. Kolsi, M. Amani, P. Estelle, G. Ahmadi, C. Kleinstreuer, J.S. Marshall, M. Siavashi, R.A. Taylor, H. Niazmand, S. Wongwises, T. Hayat, A. Kolarjijil, A. Kasaeian, I. Pop, Recent advances in modeling and simulation of nanofluid flows-part I: fundamentals and theory, *Phys. Rep.* 790 (2019) 1–48.
- [21] S. Chibowski, E.O. Mazur, J. Patkowski, Influence of ionic strength on the adsorption properties of the system dispersed aluminium oxide-polyacrylic acid, *Mater. Chem. Phys.* 93 (2005) 262–271.
- [22] A.E. Wiacek, Influence of dipalmitoylphosphatidylcholine (or dioleoylphosphatidylcholine) and phospholipase A2 enzyme on the properties of emulsions, *Journal of Colloids and Interface Science* 373 (2012) 75–83.
- [23] L.M. Corredor, M.M. Husein, B.B. Maini, Effect of hydrophobic and hydrophilic metal oxide nanoparticles on the performance of xanthan gum solutions for heavy oil recovery, *Nanomaterials* 9 (94) (2019) 1–13.
- [24] S. Shafiei-Sabet, W.Y. Hamad, S. Hatzikiriakos, Rheology of nano-crystalline cellulose aqueous suspensions, *Langmuir* 28 (49) (2012) 17124–17133.
- [25] A. Agi, R. Junin, A. Abbas, A. Gbadamosi, N.B. Azli, Effect of dynamic spreading and the disperse phase of crystalline starch nanoparticles in enhancing oil recovery at reservoir condition of a typical Sarawak oil field, *Appl. Nanosci.* 10 (1) (2020) 263–279.
- [26] W. Samutsri, M. Suphantharika, Effect of salt on pasting, thermal and rheological properties of rice starch in the presence of non-ionic and ionic hydrocolloids, *Carbohydr. Polym.* 87 (2012) 1559–1568.
- [27] A.M. Shi, D. Li, L. Wang, B. Adhikari, Suspension of vacuum-freeze dried starch nanoparticles: influence of NaCl on their rheological properties, *Carbohydr. Polym.* 94 (2013) 782–790.
- [28] L. Qiu, N. Zhu, Y. Feng, E.E. Michaelides, G. Zyla, D. Jing, X. Zhang, P.M. Norris, C.N. Markides, O. Mahian, A review of recent advances in thermophysical properties at the nanoscale: from solid state to colloids, *Phys. Rep.* 843 (2020) 1–81.
- [29] F.E. Eichie, A.E. Amalime, Evaluation of the binder effects of the gum of mucilages of *Cissus populnea* and *Acacia senegal* on the mechanical properties of paracetamol tablets, *Afr. J. Biotechnol.* 6 (19) (2007) 2208–2211.
- [30] H.Y. Kim, S.S. Park, S.T. Lim, Preparation, characterization, and utilization of starch nanoparticles, *Colloids Surf. B: Biointerfaces* 126 (2015) 607–620.
- [31] M.P. Herrera, T. Vasanathan, L. Chen, Rheology of starch nanoparticles as influenced by particle size, concentration and temperature, *Food Hydrocoll.* 66 (2017) 237–245.
- [32] H. Xiao, F. Yang, Q. Lin, Q. Zhang, L. Zhang, S. Sun, W. Han, G. Liu, Preparation and characterization of broken-rice starch nanoparticles with different sizes, *Int. J. Biol. Macromol.* 160 (2020) 437–445.
- [33] N. Yekeen, E. Padmanabhan, A.K. Idris, Synergetic effect of nanoparticles and surfactant on n-decane-water interfacial tension and bulk foam stability at high temperature, *J. Pet. Sci. Eng.* 179 (2019) 814–830.
- [34] L. Yang, W. Ji, M. Mao, J. Huang, An updated review on the properties, fabrication and application of hybrid-nanofluids along with their environmental effects, *J. Clean. Prod.* 257 (2020), 120408.
- [35] A. Bera, A. Mandal, B. Guha, Synergic effect of surfactant and salt mixture on interfacial tension reduction between crude oil and water in enhanced oil recovery, *J. Chem. Eng. Data* 59 (1) (2014) 89–96.
- [36] S.F. Sofla, M. Abbasian, M. Mirzaei, Synthesis and micellar characterization of novel pH-sensitive thiol-ended triblock copolymer via combination of RAFT and ROP processes, *International Journal of Polymeric Materials and Polymeric Biomaterial* 68 (6) (2019) 297–307.
- [37] S. Gaikwad, A. Pandit, Ultrasound emulsification: effect of ultrasound and physicochemical properties on dispersed phase volume and droplet size, *Ultrason. Sonochem.* 15 (2008) 554–563.
- [38] S. Strand, E.J. Hognesen, T. Austad, Wettability alteration of carbonates-effects of potential determining ions (Ca²⁺ and SO₄²⁻) and temperature, *Coll. Surf. A. Physicochem. Eng. Asp.* 275 (2006) 1–10.
- [39] Y. Kazemzadeh, S. Eshranghi, K. Kazemi, S. Sourani, M. Mehrabi, Y. Ahmadi, Behavior of asphaltene adsorption onto the metal oxide nanoparticles surface and its effect on the heavy oil recovery, *Ind. Eng. Chem. Res.* 54 (1) (2015) 233–239.
- [40] K. Akarzadeh, O. Sabbagh, J. Beck, W.Y. Svrcek, H.W. Yarranton, Asphaltene precipitation from bitumen diluted with n-alkanes, Paper PETSOC-2004-026-EA, Presented at Canadian International Petroleum Conference Held in Calgary, Alberta June 2004, pp. 8–14.
- [41] M. Escrochi, M. Nabipour, S. Ayatollahi, N. Mehranbod, Wettability alteration at elevated temperature: consequences of asphaltene precipitation, Paper SPE-112428-MS, Presented at SPE International Symposium and Exhibition on Formation Damage Control Held in Lafayette, Louisiana, USA, 13–15 February 2008.
- [42] N. Kumar, A. Mandal, Surfactant stabilized oil-in-water nanoemulsion: stability, interfacial tension and rheology study for enhanced oil recovery application, *Energy Fuel* 32 (6) (2018) 6452–6466.

- [43] A. Bamidele, A. Fadairo, A. Falode, Endpoint mobility ratios for vertical and horizontal wells with incidence of scale deposition, *The Open Petroleum Engineering Journal* 2 (2009) 17–23.
- [44] M. Dong, S. Ma, Q. Liu, Enhanced heavy oil recovery through interfacial instability: a study of chemical flooding for Brintnell heavy oil, *Fuel* 88 (2009) 1049–1056.
- [45] A. Agi, R. Junin, M.A. Abdullah, M.Z. Jaafar, A. Arsad, W.R. Wan Sulaiman, M.N.A. Mohd Norddin, M. Abdurrahman, A. Abbas, A. Gbadamosi, N.B. Azli, Application of polymeric nanofluid in enhancing oil recovery at reservoir condition, *J. Pet. Sci. Eng.* 194 (2020) 107476.
- [46] H. Pei, G. Zhang, J. Ge, I. Jin, C. Ma, Potential of alkaline flooding to enhance heavy oil recovery through water-in oil emulsion, *Fuel* 104 (2013) 272–278.
- [47] S. Hatscher, Schizophyllan as a Biopolymer for EOR Lab and Field Results, Winterfall, International Energy Agency (IEA), Germany, 2016.

IDN PASPOR
PASSPORT

IDN



P

NAME (LAST, FIRST / FULL NAME)

BRIDGE MEDICAL, A DIVISION OF

IDN

NET PASSPORT / PASSPORT NO.

X1158173

MUSLIM BIN DARBI ABDURRAHMAN

THE UNIVERSITY OF CHICAGO PRESS

INDONESIA

POL 1A406 - EAST OF THE RIVER

16 APR 1979

TOL. PENGELUARAN / DATE OF ISSUE

25 MAR 2021

NO. 216.

1A53BL2470-VRP



THURMAN LAMAR / PLACE OF BIRTH

DEDAP

ISS. NAME, SERIAL NO. / DATE OF EXPIRY
--

25 MAR 2026

KANTOR YANG MENGELUARKAN /
ISSUING OFFICE

PEKANBARU

P<IDNABDURRAHMAN<<MUSLIM<BIN<DARBI<<<<<<<<<<

X1158173<3IDN7904163M26032541471071604000160